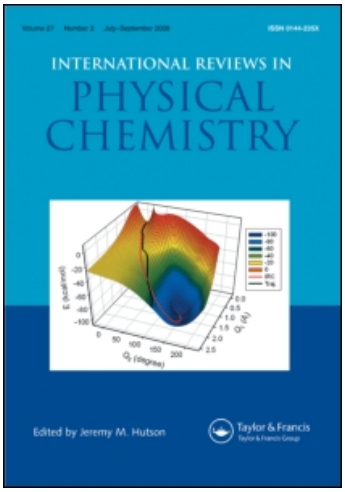

International Reviews in Physical Chemistry
Publication details, including instructions for authors and subscription information:
http://www.informaworld.com/smpp/title~content=t713724383

Molecular quantum electrodynamics in chemical physics

D. L. Andrews[a]; D. P. Craig[b]; T. Thirunamachandran[c]
[a] School of Chemical Sciences, University of East Anglia, Norwich, England [b] Research School of Chemistry, Australian National University, Canberra, Australia [c] Department of Chemistry, University College, London, England

To cite this Article Andrews, D. L. , Craig, D. P. and Thirunamachandran, T.(1989) 'Molecular quantum electrodynamics in chemical physics', International Reviews in Physical Chemistry, 8: 4, 339 — 383
To link to this Article: DOI: 10.1080/01442358909353233
URL: http://dx.doi.org/10.1080/01442358909353233

INTERNATIONAL REVIEWS IN PHYSICAL CHEMISTRY, 1989, VOL. 8, NO. 4, 339–383

Molecular quantum electrodynamics in chemical physics

by D. L. ANDREWS
School of Chemical Sciences, University of East Anglia,
Norwich NR4 7TJ, England

D. P. CRAIG
Research School of Chemistry, Australian National University,
GPO Box 4, Canberra ACT 2601, Australia

and T. THIRUNAMACHANDRAN
Department of Chemistry, University College, 20 Gordon Street,
London WC1H 0AJ, England

Molecular quantum electrodynamics (QED) is the theory of interaction of molecules with radiation. An essential feature is the application of quantum conditions to the radiation; the associated particles, which are the carriers of the momentum and energy, are photons. In QED the electrodynamic vacuum possesses zero-point energy. Fluctuations in the energy of the vacuum state are the causes of phenomena such as 'spontaneous' emission and the Lamb shift, and are the source of the virtual photons important in the understanding of intermolecular interactions. In this connection an attractive feature of the theory is its power to deal with the coupling between molecules within the same framework as radiation–molecule interactions, the molecule–molecule effects being mediated by photons, real and virtual. In this review the multipolar form of QED is described, and applications are given with some emphasis on recent work, for example three-body resonance and synergistic effects in two-photon two-molecule processes. After formulation of the theory, applications are outlined with particular reference to one- and two-photon absorption, spontaneous and stimulated emission, natural and laser-induced circular dichroism, field-induced absorption and harmonic generation. Among intermolecular interactions, accounts are given of resonance and dispersion coupling, molecule-induced circular dichroism, and cooperative two-photon absorption.

1. Introduction

Quantum electrodynamics in non-relativistic form is a theory that, in addition to many other successes, addresses at least two fundamental aspects of chemistry. One is the nature of long-range intermolecular forces, which, along with short-range interactions, determine the course of many chemical reactions, as well as the properties of condensed matter. The second is the interaction of light and other radiation with matter itself. The application to chemistry is still wider, beyond topics in this review, and has been recognized for a long time. In his Debye Lecture, Hirschfelder (1966) quoted E. Bright Wilson as saying, 'It is no longer sufficient to teach our students how to solve the Schrödinger equation, they must also know quantum electrodynamics'. Later Feynman, in his Alix Mautner Memorial Lectures, remarked that 'the theory behind chemistry is quantum electrodynamics' (Feynman 1985, p. 8).

0144–235X/89 $3·00

This review will by implication give the rationale for such comments, which reflect the broad view that chemistry includes the behaviour of molecules under all conditions, in their response to other molecules in reactions, in their coupling to radiation, and in their collective behaviour at all separation distances, from condensed matter to matter at extreme dilution. The selection of material is weighted towards recent developments, particularly in nonlinear phenomena, to supplement earlier reviews (Craig and Thirunamachandran 1982, 1986).

In current theories of the coupling of atoms and molecules to radiation, and of molecules to other molecules, there are two broad strategies. In the *semi-classical method* the atoms and molecules are treated quantum mechanically and the radiation classically. In *quantum electrodynamics* (QED) both matter and radiation are treated using quantum mechanics. The former method is more familiar. It has had notable successes, such as the calculation of the rate of light absorption through the Einstein *B*-coefficient, Placzek's account of Raman scattering, the characterization of optical rotatory strength, and circular dichroism. However, it fails to give an account, for example, of spontaneous emission (including fluorescence), the change to R^{-7} distance-dependence in the dispersion energy at long range, and the Lamb shift. It continues to be popular within the range of its proper applications.

In the semi-classical method the radiation field is treated as an external influence imposed upon the matter, and unaffected by it. It is not a part of the system being studied. Thus energy conservation does not apply in a strict sense, inasmuch as energy lost or gained by the atoms and molecules is not counterbalanced in the treatment by a gain or loss by the radiation. This creates no difficulties so long as the radiation–matter coupling is weak.

Quantum electrodynamics, having its origins in the work of Dirac (1927), and developed later by Feynman, Schwinger and Tomonaga (see Schwinger (1958) for a collection of early papers), provides at the present time the most precise description of the interaction of light and matter, correct in all applications so far made. Its principal characteristic is that light and matter together make up a closed dynamical system that is treated quantum mechanically. It lends itself naturally to descriptions in terms of photons, which are the particles associated with the quantized electromagnetic field. Energy is conserved within the closed system, being exchanged between matter and radiation: excitation of atoms and molecules is accompanied by loss of photons from the radiation and *vice versa*, satisfying energy conservation.

The particular form of QED best suited to molecular problems is the non-covariant version in the Coulomb gauge (see for example Power (1964), Healy (1982) and Craig and Thirunamachandran (1984)). In essence this allows us to separate out the Coulombic interactions within each atom or molecule. We may for that reason treat the molecular part of the coupled system of molecules and radiation as a problem already solved in ordinary molecular quantum mechanics. A second feature is that there is a choice in practice between two ways of treating the interaction between molecules and radiation: minimal coupling and multipolar coupling. They are equivalent under a canonical transformation, and each has its merits. Either allows interactions between molecules to be discussed in the same frame as interactions between molecules and radiation; by choosing the multipolar form, however, we get a beautifully simple picture. In this formulation the *only* way in which molecules couple together at distances beyond that of overlapping electron clouds is through the radiation field, mediated by an exchange of photons. Intermolecular coupling thus appears as a change of the total energy of molecules plus field, produced by molecule–radiation coupling.

Such a mediation ensures that the effects are fully retarded, namely proper allowance is made for the time of propagation (at the speed of light) for the influence of one molecule to act on another.

In both semi-classical and quantum electrodynamical methods the primitive interaction between radiation field and particles is based on the Lorentz force

$$\mathbf{F}=e(\mathbf{e}+\dot{\mathbf{r}}\times\mathbf{b}), \tag{1.1}$$

where e is the charge of the particle and $\dot{\mathbf{r}}$ its velocity; $\mathbf{e}$ and $\mathbf{b}$ are the electric and magnetic radiation field vectors. This force is a driving term in the equations of motion, together with the electrostatic forces between the particles. The contribution made by (1.1) to the coupling energy consists of both electric terms (through the electric moments of the molecular system) and magnetic terms (through the magnetic moments). Typically the latter are smaller by a factor of approximately α (the fine structure constant); so we find that the leading term involves the electric dipole, followed in the next order by electric quadrupole and magnetic dipole, and so on in higher orders.

Imposing quantum conditions on the electromagnetic field is the key step in quantum electrodynamics. In classical electromagnetism the plane-wave solutions of Maxwell's equations in free space give for the macroscopic electric field $\mathbf{E}(\mathbf{r},t)$ at position $\mathbf{r}$ and time t,

$$\mathbf{E}(\mathbf{r},t)=\mathbf{E}_0\exp[\mathrm{i}(\mathbf{k}\cdot\mathbf{r}-\omega t)], \tag{1.2}$$

where $\mathbf{k}$ is the wave-vector and ω the angular frequency. The constant amplitude $\mathbf{E}_0$ and the wave-vector $\mathbf{k}$ are unrestricted vectors. The modulus $|\mathbf{k}|=k$ is the wavenumber; $k/2\pi$ is the number of waves per unit distance along $\mathbf{k}$. Also, $k=\omega/c$, c being the velocity of light. For the purpose of quantization, the radiation field is first considered within a 'box' with periodic boundary conditions, so that the number of waves is reduced to a countable infinity. This makes possible a normalization of the states. Each combination of admissible wavenumbers, for the three directions in the box, defines a wave-vector $\mathbf{k}$, which points in the direction of propagation and has angular frequency $\omega=ck$. For each $\mathbf{k}$ there are two field modes with different polarization directions, perpendicular to $\mathbf{k}$ and to each other, which define the directions of the electric vector. Circular and elliptical polarizations are formed by linear combination.

It can be shown that the Hamiltonian for the radiation decomposes into a sum of such modes; each term has the structure of the Hamiltonian for a harmonic oscillator. Quantization is immediate. Each mode has energy levels

$$E(\mathbf{k})=(n+\tfrac{1}{2})\hbar ck, \quad n=0,1,2,\ldots\ . \tag{1.3}$$

The total is the sum over $\mathbf{k}$ and over polarization λ, and the full radiation state vector is a product of mode state vectors. The overall state of the radiation field is thus generally specified by giving the quantum number for each mode:

$$|n_1(\mathbf{k}_1,\lambda_1),n_2(\mathbf{k}_2,\lambda_2),\ldots\rangle. \tag{1.4}$$

Since the ket $|n(\mathbf{k},\lambda)\rangle$ designates a state with the energy of n photons, n is often referred to as the occupation number for the mode $(\mathbf{k},\lambda)$. In the general description of a radiation state it is conventional to include only modes with $n\neq 0$.

Some essential features of QED follow from these results. A field with no photons, the 'vacuum field', retains zero-point energy $\frac{1}{2}\hbar ck$ in each mode and has the ability to perturb molecular states. In classical electrodynamics it is possible to postulate a

molecular system isolated from radiation. The molecular states of such an isolated system would be stationary in a strict sense: an excited state would never decay. This is not true in quantum electrodynamics, nor does it agree with experiment. An excited molecule cannot be in a stationary state, because the perturbation caused by zero-point radiation is ever-present; the molecule must eventually decay under this perturbation, at a rate that is calculable, and can be shown to agree with observations of, for example, fluorescence lifetimes.

In the harmonic oscillations of a particle we are used to the idea that in the zero-point state (as in all states) the position of the particle and its conjugate momentum cannot be specified precisely at the same time. They must be seen as fluctuating about their most probable values. Similar uncertainty relations apply to the fields **e** and **b** in the modes of the electromagnetic field. Thus for the zero-point level, while the average field **e** is zero, the average of $\mathbf{e}^2$ is not; it is proportional to $\hbar ck$. These fluctuations can be seen as the underlying cause of fluorescence, for example, and of other non-classical phenomena.

Another important consequence of the presence of the zero-point energy in the electromagnetic vacuum is that over short times energy may be 'borrowed' from it to effect processes otherwise forbidden by energy conservation. The basis of this picturesque description is the time–energy uncertainty relation $\Delta E\,\Delta t \sim \frac{1}{2}\hbar$. Over short time intervals energy is not a constant even in a closed system, that is, over short times energy is not conserved. Its fluctuations cause processes such as excitation–de-excitation of electronic transitions (virtual). They account, for example, for the dispersion interactions between molecules. In that case the moment fluctuation in one molecule causes a response moment in the other, and the moments couple to give an attraction. The transitions are described as virtual, and occur by energy 'borrowing' in extremely short-term 'loans' from the zero-point energy. The interval Δt is so short that there is no sense in speaking of borrowing from individual modes. Frequencies are undefined over such periods, and the borrowing is from the entire system.

2. Formulation of QED for molecules

The quantum electrodynamical Hamiltonian for an ensemble of molecules interacting with radiation may be represented as follows:

$$H = H_{\mathrm{rad}} + \sum_{\zeta} H_{\mathrm{mol}}(\zeta) + \sum_{\zeta} H_{\mathrm{int}}(\zeta), \tag{2.1}$$

where

$$H_{\mathrm{rad}} = \frac{1}{2\varepsilon_0} \int [\mathbf{d}^{\perp 2}(\mathbf{r}) + c^2 \varepsilon_0^2 \mathbf{b}^2(\mathbf{r})]\, \mathrm{d}^3\mathbf{r}, \tag{2.2}$$

$$H_{\mathrm{mol}}(\zeta) = \frac{1}{2m} \sum_{\alpha} \mathbf{p}_{\alpha}^2(\zeta) + V(\zeta), \tag{2.3}$$

$$\begin{aligned} H_{\mathrm{int}}(\zeta) = &-\varepsilon_0^{-1} \mu(\zeta) \cdot \mathbf{d}^{\perp}(\mathbf{R}_{\zeta}) - \varepsilon_0^{-1} Q_{ij}(\zeta) \nabla_i d_j^{\perp}(\mathbf{R}_{\zeta}) - \mathbf{m}(\zeta) \cdot \mathbf{b}(\mathbf{R}_{\zeta}) \\ &+ \frac{e^2}{8m} \sum_{\alpha} [(\mathbf{q}_{\alpha}(\zeta) - \mathbf{R}_{\zeta}) \times \mathbf{b}(\mathbf{R}_{\zeta})]^2 \\ &+ \ldots + \frac{1}{2\varepsilon_0} \int |\mathbf{p}_{\zeta}^{\perp}(\mathbf{r})|^2\, \mathrm{d}^3\mathbf{r}. \end{aligned} \tag{2.4}$$

The first term in (2.1) is the radiation Hamiltonian, and its explicit expression (2.2) in terms of the transverse electric displacement field operator $\mathbf{d}^{\perp}(\mathbf{r})$ and the magnetic field operator $\mathbf{b}(\mathbf{r})$ is the operator equivalent of the classical expression for electromagnetic energy. The transverse displacement vector rather than the electric field must appear in the multipolar method to keep variables to the canonically conjugate form. The vector $\varepsilon_0^{-1}\mathbf{d}^{\perp}(\mathbf{r})$ gives the local field felt by molecules in a sample, as modified by the polarization field due to the surrounding material. The next term given by (2.3) is the Hamiltonian in the Schrödinger representation for molecule ζ located at $\mathbf{R}_{\zeta}$. The operators $\mathbf{q}_{\alpha}$ and $\mathbf{p}_{\alpha}$ are respectively the position vector and the canonical momentum of electron α, and $V(\zeta)$ is the total intramolecular energy. The last term in (2.1) denotes the interaction between radiation and matter, expressed by (2.4) in terms of the multipole operators $\boldsymbol{\mu}(\zeta)$ (electric dipole), $\mathbf{m}(\zeta)$ (magnetic dipole), $\mathbf{Q}(\zeta)$ (electric quadrupole), etc. These are the leading terms of an infinite multipolar series. The last two terms of (2.4) represent the leading contribution to an additional diamagnetic interaction energy, and a field-independent contribution only significant for self-energy calculations; $\mathbf{p}^{\perp}$ is the transverse component of the electric polarization.

In the majority of cases the electric dipole term alone may be used without significant loss of accuracy. The justification is the fact that, provided each molecule–photon interaction is electric-dipole-allowed, the contributions from the other terms in (2.4) are much smaller, the electric quadrupole and magnetic dipole being less by a factor of approximately α (the fine structure constant) and the diamagnetic term smaller by a factor α^2. For phenomena involving molecular chirality, such as optical rotation, it is necessary to include the higher-order terms for each chiral centre.

Two key features of (2.1) should be noted. First, neither the eigenstates of H_{rad} nor those of $H_{\mathrm{mol}}(\zeta)$ are stationary states: the radiation field modifies the form of the molecular wavefunctions and the presence of matter modifies the form of the radiation wavefunctions. It is this coupling that permits the transfer of energy from one part of the system to the other. As noted in section 1, the coupling exists even in the vacuum field, with no photons present. In addition to fluorescence, it is responsible for splitting the 2^2S and 2^2P states of atomic hydrogen (the Lamb shift). The second feature is that the adoption of the multipolar form of the radiation–matter interaction results in the precise cancellation of all Coulombic terms from the Hamiltonian for the system: hence no cross-terms involving molecular pairs appear in (2.4). A result is that in this form of QED intermolecular phenomena are described in terms of coupling by virtual photons; these are photons that by definition are not observable. The formalism is at first surprising, but it accounts correctly for the nature of intermolecular forces, including retardation effects, which modify the R^{-6} dependence of the dispersion energy at short distances to the R^{-7} dependence at large separations.

The quantum mechanical operators for particle position and momentum are familiar: those for the quantum electrodynamical field operators are less so. Each of the fields is expressible as a sum over radiation modes as described in section 1:

$$\mathbf{d}^{\perp}(\mathbf{r}) = \mathrm{i}\sum_{\mathbf{k},\lambda}\left(\frac{\hbar ck\varepsilon_0}{2V}\right)^{1/2}[\mathbf{e}^{(\lambda)}(\mathbf{k})a^{(\lambda)}(\mathbf{k})\exp(\mathrm{i}\mathbf{k}\cdot\mathbf{r}) - \bar{\mathbf{e}}^{(\lambda)}(\mathbf{k})a^{\dagger(\lambda)}(\mathbf{k})\exp(-\mathrm{i}\mathbf{k}\cdot\mathbf{r})], \tag{2.5}$$

$$\mathbf{b}(\mathbf{r}) = \mathrm{i}\sum_{\mathbf{k},\lambda}\left(\frac{\hbar k}{2\varepsilon_0 cV}\right)^{1/2}[\mathbf{b}^{(\lambda)}(\mathbf{k})a^{(\lambda)}(\mathbf{k})\exp(\mathrm{i}\mathbf{k}\cdot\mathbf{r}) - \bar{\mathbf{b}}^{(\lambda)}(\mathbf{k})a^{\dagger(\lambda)}(\mathbf{k})\exp(-\mathrm{i}\mathbf{k}\cdot\mathbf{r})]. \tag{2.6}$$

Here V denotes the quantization volume, $\mathbf{e}^{(\lambda)}(\mathbf{k})$ is the polarization unit vector for the electric field in mode $(\mathbf{k}, \lambda)$; $\mathbf{b}^{(\lambda)}(\mathbf{k})$ is the corresponding unit vector for the magnetic field,

$$\mathbf{b}^{(\lambda)}(\mathbf{k}) = \hat{\mathbf{k}} \times \mathbf{e}^{(\lambda)}(\mathbf{k}). \tag{2.7}$$

Associated with the mode $(\mathbf{k}, \lambda)$ in (2.5) and (2.6) are photon creation and annihilation operators of the second-quantized formalism, $a^{\dagger(\lambda)}(\mathbf{k})$ and $a^{(\lambda)}(\mathbf{k})$ respectively. They are defined by

$$\left.\begin{aligned} a^{\dagger(\lambda)}(\mathbf{k})|n(\mathbf{k},\lambda)\rangle &= (n+1)^{1/2}|(n+1)(\mathbf{k},\lambda)\rangle, \\ a^{(\lambda)}(\mathbf{k})|n(\mathbf{k},\lambda)\rangle &= n^{1/2}|(n-1)(\mathbf{k},\lambda)\rangle. \end{aligned}\right\} \tag{2.8}$$

These operators satisfy the commutation relations

$$\left.\begin{aligned} [a^{(\lambda)}(\mathbf{k}), a^{(\lambda')}(\mathbf{k}')] &= 0, \\ [a^{\dagger(\lambda)}(\mathbf{k}), a^{\dagger(\lambda')}(\mathbf{k}')] &= 0, \\ [a^{(\lambda)}(\mathbf{k}), a^{\dagger(\lambda')}(\mathbf{k}')] &= \delta_{\mathbf{k}\mathbf{k}'}\delta_{\lambda\lambda'}. \end{aligned}\right\} \tag{2.9}$$

Using these results, it is readily shown that the radiation Hamiltonian (2.2) may be expressed alternatively in terms of the number operator $a^{\dagger}a$:

$$H_{\text{rad}} = \sum_{\mathbf{k},\lambda} [a^{\dagger(\lambda)}(\mathbf{k})a^{(\lambda)}(\mathbf{k}) + \tfrac{1}{2}]\hbar ck. \tag{2.10}$$

With the Hamiltonian given by (2.1), the time evolution of a system wavefunction $|\Psi(t)\rangle$ is determined by the time-dependent Schrödinger equation

$$i\hbar \frac{\partial}{\partial t}|\Psi(t)\rangle = H|\Psi(t)\rangle. \tag{2.11}$$

The solution of this equation is not possible in closed form except in simple cases. We assume that the coupling between matter and radiation can be treated as a perturbation on the product states of H_0, where

$$H_0 = H_{\text{rad}} + \sum_{\zeta} H_{\text{mol}}(\zeta). \tag{2.12}$$

After application of the standard methods of time-dependent perturbation theory, we obtain for the rate Γ of an optical process the Fermi golden rule

$$\Gamma = \frac{2\pi}{\hbar}|M_{\text{fi}}|^2\rho, \tag{2.13}$$

where ρ is a density of states for the process. Typically ρ is the density of states of the radiation field in the energy region of the process. The transition matrix element M_{fi} connecting the initial state $|\text{i}\rangle$ and the final state $|\text{f}\rangle$ is given by

$$\begin{aligned} M_{\text{fi}} = \langle \text{f}|H_{\text{int}}|\text{i}\rangle &+ \sum_{I} \frac{\langle \text{f}|H_{\text{int}}|I\rangle\langle I|H_{\text{int}}|\text{i}\rangle}{E_{\text{i}} - E_I} \\ &+ \sum_{I,II} \frac{\langle \text{f}|H_{\text{int}}|II\rangle\langle II|H_{\text{int}}|I\rangle\langle I|H_{\text{int}}|\text{i}\rangle}{(E_{\text{i}} - E_I)(E_{\text{i}} - E_{II})} + \ldots \quad . \end{aligned} \tag{2.14}$$

Here all states and energies are eigenstates and eigenvalues of H_0 and thus relate to the total system comprising both radiation and matter. The summations over the virtual (intermediate) states $|I\rangle$, $|II\rangle$, are taken over all such states, excluding $|\text{i}\rangle$ and $|\text{f}\rangle$.

Since the total system is closed, the initial and final energies E_i and E_f must always be equal (to within a quantum uncertainty limit). In the electric dipole approximation the interaction Hamiltonian is linear in the displacement vector field, and it follows from (2.5) that each Dirac bracket in (2.14) is associated with the creation or annihilation of one photon. Hence the mth term in (2.14), corresponding to the mth order in perturbation theory, is the dominant term for an m-photon process. Similar remarks apply when electric quadrupole and magnetic dipole couplings are included in the calculations. Exceptions occur in cases where quadratic terms such as the diamagnetic term in (2.4) are significant.

It should be noted that the absence of electrostatic interactions between molecules in the multipolar formalism means that there is no term in (2.1) representing interactions with an applied *static* electric or magnetic field. While such interactions could in principle be modelled by summing the couplings of each sample molecule with each constituent particle of the field source, it is often simpler in practice to 'dress' the molecular states with a suitable time-independent perturbation. In the case of a static electric displacement field $\mathbf{D}$ these dressed states are given by

$$|r'\rangle = |r\rangle - \varepsilon_0^{-1} \sum_{s \neq r} (\boldsymbol{\mu}^{rs} \cdot \mathbf{D}) E_{rs}^{-1} |s\rangle + \ldots, \tag{2.15}$$

where $|r\rangle$ and $|s\rangle$ represent eigenstates of the conventional Hamiltonian operator H_{mol} in the absence of the applied electric field, and E_{rs} is the difference between the corresponding zeroth-order energies $E_r - E_s$; $\boldsymbol{\mu}^{sr}$ is the transition electric dipole moment for the $|s\rangle \leftarrow |r\rangle$ transition. Any optical process in the presence of a static electric field may then be modelled using (2.13) and (2.14) with the dressed states as basis.

3. One-photon absorption

Quantum electrodynamics was first applied by Dirac (1927) to the absorption of a photon by an atom or molecule. This is the simplest interaction of radiation with matter, and the one most familiar as the primary origin of colour. It is also central to chemistry through almost every type of spectroscopy and photochemistry. One of the signal successes of the theory is that its results apply not only to light in the visible range, but also across the entire electromagnetic spectrum. In many cases where the transition electric dipole moment $\boldsymbol{\mu}$ is non-zero, or at least not very small, it is adequate to employ the electric dipole approximation to describe the allowed transitions. This approximation holds when the wavelength of the radiation is long compared with molecular dimensions; the electric field in the region occupied by the molecule is then essentially constant, and the coupling between the molecule at $\mathbf{R}$ and the field is $-\varepsilon_0^{-1} \boldsymbol{\mu} \cdot \mathbf{d}(\mathbf{R})$.

To calculate the matrix element for the process, as required for application of the Fermi rule (2.13), we first specify the initial and final states of the system. Initially the molecule is in the ground state, and the state of an idealized monochromatic beam is given by the number of photons in the single mode $(\mathbf{k}, \lambda)$. This state is represented by

$$|\mathrm{i}\rangle = |E_0\rangle |n(\mathbf{k}, \lambda)\rangle. \tag{3.1}$$

In the final state the molecule is in an excited state $|E_m\rangle$ and the radiation field has lost one photon. Thus

$$|\mathrm{f}\rangle = |E_m\rangle |(n-1)(\mathbf{k}, \lambda)\rangle. \tag{3.2}$$

Energy is conserved overall:

$$E_m - E_0 = E_{m0} = \hbar ck. \tag{3.3}$$

We digress at this stage to introduce time-ordered graphs that enable the matrix elements to be calculated easily. Although the graphical method is not essential for calculating first-order matrix elements, we introduce some of the basic notions now and discuss further aspects later when dealing with higher-order processes. The graph for single-photon absorption is shown in figure 1. In interpreting this graph time flows upwards, and the vertical line represents the changes in the molecular state during the process. The wavy line stands for a photon. The intersection of the vertical line and the wavy line represents the coupling between photon and molecule, and is usually referred to as an interaction vertex. Although the radiation field may contain many photons, it is conventional to show only the changes in the field. The initial and final states can be read with the aid of horizontal lines (not shown) below and above the interaction vertex; the energies follow immediately.

The matrix element for single-photon absorption is

$$M_{\mathrm{fi}} = \langle \mathrm{f}| -\varepsilon_0^{-1}\boldsymbol{\mu}\cdot\mathbf{d}(\mathbf{R})|\mathrm{i}\rangle$$

$$= -\mathrm{i}\left(\frac{n\hbar ck}{2\varepsilon_0 V}\right)^{1/2} \mathbf{e}^{(\lambda)}(\mathbf{k})\cdot\boldsymbol{\mu}^{m0}\exp(\mathrm{i}\mathbf{k}\cdot\mathbf{R}), \tag{3.4}$$

where the expansion (2.5) has been used for $\mathbf{d}$. The absorption rate is found from the Fermi rule as

$$\Gamma = \frac{2\pi}{\hbar}|M_{\mathrm{fi}}|^2\rho$$

$$= \frac{2\pi}{\hbar}\rho\frac{n\hbar ck}{2\varepsilon_0 V}|\mathbf{e}^{(\lambda)}\cdot\boldsymbol{\mu}^{m0}|^2. \tag{3.5}$$

This rate expression is easily modified to take account of the physically more realistic case where the sample contains a large number N of molecules. We then have for the total rate

$$\Gamma = \frac{2\pi}{\hbar}\rho\frac{n\hbar ck}{2\varepsilon_0 V}\sum_{\zeta}^{N}|\mathbf{e}^{(\lambda)}(\mathbf{k})\cdot\boldsymbol{\mu}^{m0}(\zeta)|^2, \tag{3.6}$$

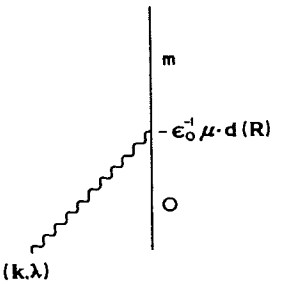

Figure 1. Time-ordered diagram for one-photon absorption with electric dipole coupling.

where ζ is the molecular label. In a fluid phase the molecules are randomly oriented with respect to the incident beam, and an orientational average of (3.6) is required. This gives

$$\langle \Gamma \rangle = \frac{2\pi N}{3\hbar} \rho \frac{n\hbar ck}{2\varepsilon_0 V} |\mu^{m0}|^2. \tag{3.7}$$

The rate (3.7) must finally be related to the intensity of the incident beam through ρ, the density of states. The transition is caused only by frequencies close to the resonant frequency ck, within a span set by the lifetime τ of the molecular state $|m\rangle$. Typically, for $\tau \sim 10^{-9}$ s, the circular frequency width is 8×10^7 Hz or 3×10^{-3} cm^{-1}. In terms of $\mathscr{I}(\omega)$, the radiant energy density per unit frequency, we have

$$\rho = \frac{\mathscr{I}(\omega) V}{2\pi n \hbar^2 \omega}, \tag{3.8}$$

so that

$$\begin{aligned} \langle \Gamma \rangle &= \frac{N \mathscr{I}(\omega)}{6\varepsilon_0 \hbar^2} |\mu^{m0}|^2 \\ &= NB\mathscr{I}(\omega), \end{aligned} \tag{3.9}$$

where

$$B = \frac{1}{6\varepsilon_0 \hbar^2} |\mu^{m0}|^2. \tag{3.10}$$

is the Einstein B-coefficient. The rate (3.9) is independent of the polarization of the incident beam, as a result of the orientational averaging leading to (3.7) and the scalar character of $|\mu^{m0}|^2$.

4. Spontaneous emission

An isolated atom or molecule in an excited state does not remain excited indefinitely but decays to the ground state with the emission of a photon. To contrast with *stimulated* emission (*vide infra*) this process in any region of the electromagnetic spectrum is referred to as *spontaneous*. While a molecular energy level is a stationary state of the free-molecule Hamiltonian, it is not stationary under the complete Hamiltonian, which must always include the radiation field. Spontaneous emission cannot be understood within the semi-classical framework since there is no external radiation field to perturb the atom or molecule. The excited state of a molecule is then a genuine stationary state of the system and there is no radiative decay. Before QED, spontaneous emission was understood only at a statistical level, through Einstein's theory of the equilibrium balance required between absorption and the processes of stimulated and spontaneous emission. The microscopic mechanism of the latter process remained mysterious. From a quantum electrodynamical point of view, the electromagnetic vacuum exhibits zero-point fluctuations and can interact with an excited molecule, leading to radiative decay. The calculation of the spontaneous emission rate is straightforward and was one of the striking early successes of QED.

The initial state of the system is $|E_m; 0\rangle$ where the molecule is in the mth level and the radiation field is the vacuum. The density of states required for rate calculation by the Fermi rule is now associated with the final state $|E_0; 1(\mathbf{k}, \lambda)\rangle$. This state is highly degenerate because the emitted photon can occupy one of the large number of modes

with different directions of propagation and polarization, all with energies of approximately E_{m0}. By counting the number of modes with wavevector between $\mathbf{k}$ and $\mathbf{k}+\mathrm{d}\mathbf{k}$, the density of final states can be obtained (Heitler 1954) as

$$\rho = \frac{k^2\,\mathrm{d}\Omega}{(2\pi)^3\hbar c}V. \tag{4.1}$$

In the electric dipole approximation the matrix element for emission is

$$\begin{aligned} M_{\mathrm{fi}} &= \langle 1(\mathbf{k},\lambda); E_0|-\varepsilon_0^{-1}\boldsymbol{\mu}\cdot\mathbf{d}(\mathbf{R})|E_m;0\rangle \\ &= \mathrm{i}\left(\frac{\hbar ck}{2\varepsilon_0 V}\right)^{1/2}\bar{\mathbf{e}}^{(\lambda)}(\mathbf{k})\cdot\boldsymbol{\mu}^{0m}\exp(\mathrm{i}\mathbf{k}\cdot\mathbf{R}). \end{aligned} \tag{4.2}$$

The total rate for emission is found from the Fermi rule using (4.1) and (4.2), integrating over all directions of $\hat{\mathbf{k}}$, and summing over polarizations. We then have

$$\Gamma = \frac{\omega^3}{3\pi\varepsilon_0\hbar c^3}|\boldsymbol{\mu}^{0m}|^2. \tag{4.3}$$

which is equal to the Einstein A-coefficient, as found by the energy balance argument mentioned earlier.

The rate (4.3) applies to emission in free space. If the molecule is contained in a cavity, the rate can be radically modified because of changes in the boundary conditions. An interesting example is that in which the transition wavelength for emission is greater than the cavity size; spontaneous emission is then substantially inhibited. Such changes have been observed in Rydberg transitions of alkali atoms (Hulet *et al.* 1985).

5. Stimulated emission

Emission of light from an excited atom or molecule may occur by a second route. When a radiation field is incident on an excited system, at a frequency equal to the transition frequency, it induces downward transitions at the same frequency. This process, called induced or stimulated emission, is the inverse of absorption, and is well known as the mechanism for laser action.

In absorption the transition may be represented as

$$|E_m;(n-1)(\mathbf{k},\lambda)\rangle \leftarrow |E_0;n(\mathbf{k},\lambda)\rangle, \tag{5.1}$$

whereas stimulated emission corresponds to

$$|E_0;(n+1)(\mathbf{k},\lambda)\rangle \leftarrow |E_m;n(\mathbf{k},\lambda)\rangle. \tag{5.2}$$

The calculation of the stimulated emission rate follows the same lines as that of the absorption rate. The result is

$$\langle \Gamma_{\mathrm{stimulated}}\rangle = N_m B\mathscr{I}(\omega), \tag{5.3}$$

where N_m is the number of molecules initially in the excited state, B is the Einstein coefficient and $\mathscr{I}(\omega)$ is the radiant energy density per unit frequency. In terms of radiation modes (section 2), stimulated emission goes into the mode, or modes, already occupied by the stimulating beam, and increases the occupation number of those modes. Its direction and polarization are the same as the stimulating beam, giving rise to intense and tightly collimated emission. In contrast, spontaneous emission is random in direction and polarization. It is incoherent, being produced by a large number of independent emitters. The emission events are uncorrelated.

Coherence properties in QED are different from those of classical theory, in which the phase of a wave can be specified simultaneously with its energy. Two classical beams able to exhibit interference by superposition are said to be coherent. To take an example, plane-wave radiation with N emitters that is perfectly in phase at some point gives an electric field (as in (1.2)) that is N times that of a single emitter, and an intensity going as N^2. In incoherent radiation the proportionality is with N. In the quantum theory the operators for phase angle and occupation number do not commute (Carruthers and Nieto 1968). Application of the uncertainty principle gives the result that if the occupation number of a mode is specified ($n>0$), so that the energy is known exactly, the phase is random. The quantal state that approaches most closely the classical electromagnetic wave is the so-called coherent state (Glauber 1963). Both phase and amplitude have some uncertainty. For large occupation number, coherent states are states of minimum possible uncertainty for measurements of occupation number and phase angle. Moreover, the property of minimum uncertainty is constant over time; the dispersion in the field remains constant and is independent of the field amplitude.

In lasers a system of identical absorbers is pumped, typically by broadband light absorption, to give a high population of excited atoms or molecules. There is decay by stimulated emission, giving radiation with the characteristics of the coherent state.

6. Natural circular dichroism

The calculation of the absorption rate given in section 3 is easily extended to deal with circular dichroism, namely the differential rate of absorption of left- and right-circularly polarized light. In optically active molecules, some transitions are *both* electric- and magnetic-dipole-allowed. To calculate the rates, it is then necessary to take into account the couplings of the molecular transition moments to both electric and magnetic fields. The transition amplitude is a superposition of electric and magnetic dipole amplitudes. For randomly oriented systems, the electric-dipole–magnetic-dipole interference term depends on the handedness of the circularly polarized incident beam. Circular dichroism arises from this interference (Power and Thirunamachandran 1974, 1986).

Let a photon of mode ($\mathbf{k}$, L/R) (where L and R represent left- and right-circular polarization) be absorbed by a molecule at $\mathbf{R}$. For the molecular transition $|m\rangle \leftarrow |0\rangle$, energy is conserved overall, so that $E_{m0}=\hbar ck$. For simplicity the molecular states are assumed to be non-degenerate. With

$$|\mathrm{i}\rangle = |E_0; n(\mathbf{k}, \mathrm{L/R})\rangle, \tag{6.1}$$

$$|\mathrm{f}\rangle = |E_m; (n-1)(\mathbf{k}, \mathrm{L/R})\rangle \tag{6.2}$$

as initial and final states, it is straightforward to calculate the matrix element for absorption. The coupling between the molecule and the radiation field is now given by

$$H_{\mathrm{int}} = -\varepsilon_0^{-1}\boldsymbol{\mu}\cdot\mathbf{d}(\mathbf{R}) - \mathbf{m}\cdot\mathbf{b}(\mathbf{R}). \tag{6.3}$$

where $\mathbf{m}$ is the magnetic dipole moment operator. The diagram for electric dipole absorption given in section 3 is now supplemented by that for magnetic dipole

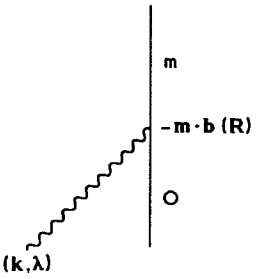

Figure 2. Time-ordered diagram for one-photon absorption with magnetic dipole coupling.

absorption (figure 2), the complete matrix element being the sum of terms from the two diagrams. Using the expansions for **d** and **b**, we obtain

$$M_{fi}^{L/R} = -i\left(\frac{n\hbar ck}{2\varepsilon_0 V}\right)^{1/2} \mathbf{e}^{(L/R)}(\mathbf{k}) \cdot \left(\boldsymbol{\mu}^{m0} \mp \frac{i}{c}\mathbf{m}^{m0}\right) \exp(i\mathbf{k}\cdot\mathbf{R}), \tag{6.4}$$

where the upper and lower signs hold for left- and right-circularly polarized light respectively. The absorption rate follows in the usual way from the Fermi rule:

$$\langle \Gamma^{L/R} \rangle = \frac{2\pi N}{3\hbar} \frac{n\hbar ck}{2\varepsilon_0 V} \rho \left| \boldsymbol{\mu}^{m0} \mp \frac{i}{c}\mathbf{m}^{m0} \right|^2. \tag{6.5}$$

It is readily seen from (6.5) that the electric–magnetic cross-term depends on the handedness of light. This cross-term provides the leading contribution to circular dichroism,

$$\langle \Gamma^{L} \rangle - \langle \Gamma^{R} \rangle = -i\frac{8\pi N}{3\hbar c} \frac{n\hbar ck}{2\varepsilon_0 V} \rho \boldsymbol{\mu}^{0m} \cdot \mathbf{m}^{m0}$$

$$< \frac{2N\mathcal{I}(\omega)}{3\hbar^2 c\varepsilon_0} R^{m0}, \tag{6.6}$$

where $\mathcal{I}(\omega)$ is the radiant energy density per unit frequency and R^{m0} is the optical rotatory strength defined by

$$R^{m0} = \mathrm{Im}\, \boldsymbol{\mu}^{m0} \cdot \mathbf{m}^{m0}. \tag{6.7}$$

The scalar product of the polar and axial vectors in (6.7) behaves as a scalar under rotations, but changes sign under inversion and reflection. It is thus a pseudoscalar and takes opposite signs for enantiomers, as does circular dichroism itself.

We have seen in this section how a simple extension of the electric dipole approximation leads to a direct calculation of circular dichroism using QED. The inclusion of the magnetic dipole coupling corresponds to the inclusion of the first derivative of the vector potential in the minimal-coupling formalism. For consistency it would therefore be necessary to include electric quadrupole coupling as well. However, a calculation similar to the one above shows that the electric-dipole–electric-quadrupole interference term averages to zero in an isotropic system (Craig and Thirunamachandran 1984).

7. Laser-induced circular dichroism

With the arrival of lasers as sources of coherent radiation of high intensity, it has become possible to observe a new class of chiroptical processes. An example is laser-induced dichroism (Delsart and Keller 1978). This is the differential absorption of left- and right-circularly polarized light by an optically inactive (achiral) medium irradiated by an intense beam of circularly polarized radiation. The frequency of the intense beam (pump) is non-resonant with any of the transition frequencies of the achiral molecule. The physical picture of laser-induced circular dichroism is that the intense beam of circularly polarized light induces a chirality in the achiral molecule. This is then probed by a second beam (probe) of circularly polarized light. The differential absorption rate is calculated straightforwardly using QED (Thirunamachandran 1979).

Consider the transition $|m\rangle \leftarrow |0\rangle$ of the achiral molecule. Let the mode of the intense beam be $(\mathbf{k}, \mathrm{L})$ and that of the probe beam be $(\mathbf{k}', \mathrm{L/R})$. The frequency of the probe beam is chosen to be resonant with that of the molecular transition, namely $E_{m0} = \hbar ck'$. In the transition the probe beam loses one photon; the pump beam, however, remains unchanged overall, though it may have lost or gained a virtual photon in the intermediate states of the process. In the leading order of perturbation theory the pump beam is not coupled to the molecule: the molecule simply absorbs a photon from the probe beam. The time-ordered diagram is the same as that for one-photon absorption (figure 1), and the first-order matrix element in the electric dipole approximation is

$$M_1^{\mathrm{L/R}} = -\mathrm{i}\left(\frac{n'\hbar ck'}{2\varepsilon_0 V}\right)^{1/2} \mathbf{e}^{(\mathrm{L/R})}(\mathbf{k}') \cdot \boldsymbol{\mu}^{m0}. \tag{7.1}$$

The term for the coupling of the pump beam to the molecule is of third order in perturbation theory. It corresponds overall to the scattering of a photon from the pump beam and the absorption of a photon from the probe beam. Several different types of intermediate state contribute to the third-order matrix element. The time-ordered diagrams provide a convenient way of ensuring that all relevant intermediate states are taken into account. A typical diagram for the third-order process is shown in figure 3. It represents the sequence of absorption of a photon of mode $(\mathbf{k}', \mathrm{L/R})$ followed by absorption and emission of a photon of mode $(\mathbf{k}, \mathrm{L})$. For this sequence the molecule undergoes excitation to the intermediate states $|E_r\rangle$ and $|E_s\rangle$ and finally reaches the excited state $|E_m\rangle$ for the overall transition $m \leftarrow 0$. In the intermediate states energy is not conserved; there is energy conservation only between initial and final states. For the diagram shown in figure 3 the states are

$$\left.\begin{aligned} |\mathrm{i}\rangle &= |E_0; n(\mathbf{k}, \mathrm{L}), n'(\mathbf{k}', \mathrm{L/R})\rangle, \\ |I\rangle &= |E_r; n(\mathbf{k}, \mathrm{L}), (n'-1)(\mathbf{k}', \mathrm{L/R})\rangle, \\ |II\rangle &= |E_s; (n-1)(\mathbf{k}, \mathrm{L}), (n'-1)(\mathbf{k}', \mathrm{L/R})\rangle, \\ |\mathrm{f}\rangle &= |E_m; n(\mathbf{k}, \mathrm{L}), (n'-1)(\mathbf{k}', \mathrm{L/R})\rangle, \end{aligned}\right\} \tag{7.2}$$

and the corresponding energies are

$$\left.\begin{aligned} E_{\mathrm{i}} &= E_0 + n\hbar\omega + n'\hbar\omega', \\ E_I &= E_r + n\hbar\omega + (n'-1)\hbar\omega', \\ E_{II} &= E_s + (n-1)\hbar\omega + (n'-1)\hbar\omega', \\ E_{\mathrm{f}} &= E_m + n\hbar\omega + (n'-1)\hbar\omega'. \end{aligned}\right\} \tag{7.3}$$

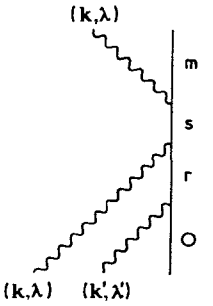

Figure 3. Typical third-order graph for laser-induced circular dichroism.

Using the expansion (2.5) for the **d**-field, the contribution to the matrix element from the diagram in figure 3 is easily written down:

$$-\mathrm{i}\left(\frac{n'\hbar ck'}{2\varepsilon_0 V}\right)^{1/2}\frac{n\hbar ck}{2\varepsilon_0 V}\bar{e}_i^{(\mathrm{L})}(\mathbf{k})e_j^{(\mathrm{L})}(\mathbf{k})e_k^{(\mathrm{L/R})}(\mathbf{k}')\sum_{r,s}\frac{\mu_i^{ms}\mu_j^{sr}\mu_k^{r0}}{(E_{sm}-\hbar\omega)(E_{r0}-\hbar\omega')}. \tag{7.4}$$

The total contribution to the third-order matrix element is obtained from the diagrams corresponding to all possible time-ordered sequences. For the present case there are six diagrams in all. The total third-order matrix element is

$$M_3^{\mathrm{L,L/R}}=-\mathrm{i}\left(\frac{n'\hbar ck'}{2\varepsilon_0 V}\right)^{1/2}\frac{n\hbar ck}{2\varepsilon_0 V}\bar{e}_i^{(\mathrm{L})}(\mathbf{k})e_j^{(\mathrm{L})}(\mathbf{k})e_k^{(\mathrm{L/R})}(\mathbf{k}')\beta_{ijk}^{m0}, \tag{7.5}$$

where the magnitude depends on the third-rank tensor

$$\begin{aligned}\beta_{ijk}=\sum_{r,s}\Bigg[&\frac{\mu_i^{ms}\mu_j^{sr}\mu_k^{r0}}{E_{sm}-\hbar\omega)(E_{r0}-\hbar\omega')}+\frac{\mu_j^{ms}\mu_i^{sr}\mu_k^{r0}}{(E_{sm}+\hbar\omega)(E_{r0}-\hbar\omega')}\\&+\frac{\mu_j^{ms}\mu_k^{sr}\mu_i^{r0}}{(E_{sm}+\hbar\omega)(E_{r0}+\hbar\omega)}+\frac{\mu_i^{ms}\mu_k^{sr}\mu_j^{r0}}{(E_{sm}-\hbar\omega)(E_{r0}-\hbar\omega)}\\&+\frac{\mu_k^{ms}\mu_i^{sr}\mu_j^{r0}}{E_{s0}(E_{r0}-\hbar\omega)}+\frac{\mu_k^{ms}\mu_j^{sr}\mu_i^{r0}}{E_{s0}(E_{r0}+\hbar\omega)}\Bigg].\end{aligned} \tag{7.6}$$

The total absorption rate is

$$\Gamma^{\mathrm{L,L/R}}=\frac{2\pi}{\hbar}|M_1^{\mathrm{L/R}}+M_3^{\mathrm{L,L/R}}|^2\rho, \tag{7.7}$$

from which it is seen that the leading contribution to the differential absorption rate arises from the interference of first- and third-order terms. We find

$$\langle\Gamma^{\mathrm{LL}}\rangle-\langle\Gamma^{\mathrm{LR}}\rangle=\frac{1}{12\varepsilon_0^2\hbar c}I\mathscr{S}'(\omega')(\hat{\mathbf{k}}\cdot\hat{\mathbf{k}}')(\mu_\lambda^{m0}\beta_{\mu\lambda\mu}^{m0}-\mu_\lambda^{m0}\beta_{\lambda\mu\mu}^{m0}), \tag{7.8}$$

where I is the irradiance of the beam, $\mathscr{I}'(\omega')$ is the energy density per unit frequency of the probe beam and $\hat{\mathbf{k}}$ is the unit vector along $\mathbf{k}$. It is convenient to express the laser-induced circular dichroism as a differential ratio

$$\Delta = \frac{\langle \Gamma^{LL} \rangle - \langle \Gamma^{LR} \rangle}{\langle \Gamma^{LL} \rangle + \langle \Gamma^{LR} \rangle}$$
$$= \frac{I}{4\varepsilon_0 c}(\hat{\mathbf{k}} \cdot \hat{\mathbf{k}}') \frac{\mu_\lambda^{m0} \beta_{\mu\lambda\mu}^{m0} - \mu_\lambda^{m0} \beta_{\lambda\mu\mu}^{m0}}{|\boldsymbol{\mu}^{m0}|^2}. \tag{7.9}$$

The quantity Δ is linearly dependent on the irradiance of the pump beam and on the cosine of the angle between the directions of propagation of the two beams. In natural circular dichroism (section 6) the differential rate depends on the pseudoscalar $\boldsymbol{\mu} \cdot \mathbf{m}$. In laser-induced circular dichroism it depends on the contracted product of the transition moment and the β-tensor, with sign depending on the relative handedness of the two beams. A change of helicity of the pump beam leads to a change in the sign of $\mathbf{k}$ in (7.9), resulting in a change of sign in Δ.

8. Two-photon absorption

Two-photon optical absorption measurements first became possible after the application of lasers as light sources. They are important because they provide information complementary to one-photon absorption. The selection rules for two-photon absorption are in general different, in the same way as vibrational Raman selection rules differ from infrared. For example, in centrosymmetric molecules $g \leftrightarrow u$ transitions are one-photon electric-dipole-allowed but two-photon forbidden; $g \leftrightarrow g$ and $u \leftrightarrow u$ are two-photon allowed but one-photon forbidden. In the language of perturbation theory, two-photon absorption is a second-order process and the matrix element involves a non-stationary intermediate state (i.e. a state for which energy is not conserved). The rate of two-photon absorption, and thus the absorption intensity, is many orders of magnitude less than one-photon absorption with typical laboratory sources. The absorption rate is proportional to the square of the intensity.

Let us first consider the case of absorption of two photons from one beam. The initial and final states are

$$|\mathrm{i}\rangle = |E_0; n(\mathbf{k}, \lambda)\rangle, \tag{8.1}$$

$$|\mathrm{f}\rangle = |E_m; (n-2)(\mathbf{k}, \lambda)\rangle. \tag{8.2}$$

The intermediate state is of the form

$$|I\rangle = |E_r; (n-1)(\mathbf{k}, \lambda)\rangle, \tag{8.3}$$

where the molecule is transiently in a state $|E_r\rangle$ and the field has lost one photon. The transitions $|I\rangle \leftarrow |\mathrm{i}\rangle$ and $|\mathrm{f}\rangle \leftarrow |I\rangle$ are not real processes in the technical sense. Energies are *not* conserved individually in these steps, that is $E_{r0} \neq \hbar ck$ and $|E_{mr}| \neq \hbar ck$. The intermediate steps are usually referred to as virtual processes and the intermediate states as virtual states. The real and identifiable process is the overall transition $|E_m\rangle \leftarrow |E_0\rangle$ with energy conservation $E_{m0} = 2\hbar ck$. The time-ordered diagram for two-photon absorption from a single beam is shown in figure 4. The matrix element for the process is

$$M_{\mathrm{fi}} = \frac{\hbar ck}{2\varepsilon_0 V}[n(n-1)]^{1/2} e_i e_j \sum_r \frac{\mu_i^{mr} \mu_j^{r0}}{E_{r0} - \hbar\omega}, \tag{8.4}$$

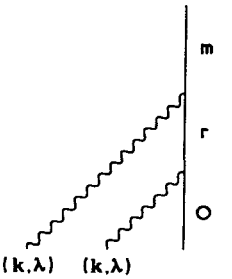

Figure 4. Time-ordered graph for absorption of two photons from one beam.

where the photon mode labels have been suppressed. Since $e_i e_j$ is (i,j)-symmetric, only the (i,j)-symmetric part of the molecular tensor in (8.4) contributes. Thus

$$M_{\mathrm{fi}}=\frac{1}{2}\frac{\hbar ck}{2\varepsilon_0 V}[n(n-1)]^{1/2}e_i e_j\sum_r\left(\frac{\mu_i^{mr}\mu_j^{r0}}{E_{r0}-\hbar\omega}+\frac{\mu_j^{mr}\mu_i^{r0}}{E_{r0}-\hbar\omega}\right). \tag{8.5}$$

The two-photon absorption rate for the case where the absorbers are in the fluid phase is now obtained by orientational averaging of the tensor products (Andrews and Thirunamachandran 1977). The result is

$$\langle\Gamma\rangle=\frac{2\pi N}{\hbar}\left(\frac{\hbar ck}{4\varepsilon_0 V}\right)^2\frac{\rho n(n-1)}{15}[(2|\mathbf{e}\cdot\mathbf{e}|^2-1)\alpha_{\lambda\lambda}^{m0}(\omega,\omega)\bar{\alpha}_{\mu\mu}^{m0}(\omega,\omega)$$
$$-(|\mathbf{e}\cdot\mathbf{e}|^2-3)\alpha_{\lambda\mu}^{m0}(\omega,\omega)\bar{\alpha}_{\lambda\mu}^{m0}(\omega,\omega)] \tag{8.6}$$

where

$$\alpha_{\lambda\mu}^{m0}(\omega,\omega)=\sum_r\left(\frac{\mu_\lambda^{mr}\mu_\mu^{r0}}{E_{r0}-\hbar\omega}+\frac{\mu_\mu^{mr}\mu_\lambda^{r0}}{E_{r0}-\hbar\omega}\right). \tag{8.7}$$

The rate (8.6) depends on the square of the beam intensity. We have seen in (3.8) that the radiant energy density per unit frequency, $\mathscr{I}(\omega)$, is given by

$$\mathscr{I}(\omega)=\frac{2\pi n\hbar^2\omega}{V}\rho. \tag{8.8}$$

By defining the irradiance

$$I=\frac{n\hbar c\omega}{V}, \tag{8.9}$$

we have for the rate,

$$\langle\Gamma\rangle=N\frac{n-1}{n}I\mathscr{I}(\omega)B^{(2)}, \tag{8.10}$$

where here

$$B^{(2)}=\frac{1}{240\hbar^2 c\varepsilon_0^2}[(2|\mathbf{e}\cdot\mathbf{e}|^2-1)\alpha_{\lambda\lambda}^{m0}(\omega,\omega)\bar{\alpha}_{\mu\mu}^{m0}(\omega,\omega)$$
$$+(|\mathbf{e}\cdot\mathbf{e}|^2-3)\alpha_{\lambda\mu}^{m0}(\omega,\omega)\bar{\alpha}_{\lambda\mu}^{m0}(\omega,\omega)]. \tag{8.11}$$

The coefficient $B^{(2)}$ for two-photon absorption is analogous to the Einstein B-coefficient in (3.10). It is of fourth power in the dipole transition moments.

The term $(n-1)/n$ in (8.10) giving the dependence of the rate on the radiation mode occupation number applies to absorption from a beam for which the occupation number n is exactly known. If the state of the radiation field is specified in some other way, the expression (8.10) is generalized to

$$\langle \Gamma \rangle = N\bar{I}\bar{\mathscr{F}}(\omega) g^{(2)} B^{(2)}, \tag{8.12}$$

where

$$g^{(2)} = \frac{\langle n(n-1) \rangle}{\langle n \rangle^2}, \tag{8.13}$$

and $\bar{I}$ and $\bar{\mathscr{F}}$ are mean quantities. The expectation values in angular brackets involve the number operator $a^\dagger a$, instead of its eigenvalues as in (8.10). The factor $g^{(2)}$ is a measure of the coherence properties of the radiation mentioned in section 5; it is usually referred to as the degree of second-order coherence. For number states, as in (8.10), it is $(n-1)/n$. For coherent states $g^{(2)}=1$, and for chaotic states produced, for example, by thermal sources $g^{(2)}=2$.

The discussion is easily extended to include two-photon absorption from two beams. With tunable lasers, two-photon absorption from two beams is experimentally accessible. Such experiments provide more information than from a single beam. Let the modes of the two beams be $(\mathbf{k}, \lambda)$ and $(\mathbf{k}', \lambda')$, and the molecular transition of interest be $|m\rangle \leftarrow |0\rangle$. It is assumed that one photon from each mode is absorbed so that $E_{m0} = \hbar ck + \hbar ck'$. It is evident that two types of intermediate states are possible, depending on whether a photon $(\mathbf{k}, \lambda)$ or $(\mathbf{k}', \lambda')$ is absorbed first. In terms of time-ordered diagrams, the two cases correspond to two different time sequences as shown in figure 5.

The matrix element for absorption of two photons is

$$M_{fi} = \left(\frac{n\hbar ck}{2\varepsilon_0 V}\right)^{1/2} \left(\frac{n'\hbar ck'}{2\varepsilon_0 V}\right)^{1/2} e_i' e_j \sum_r \left(\frac{\mu_i^{mr}\mu_j^{r0}}{E_{r0} - \hbar\omega} + \frac{\mu_j^{mr}\mu_i^{r0}}{E_{r0} - \hbar\omega'} \right), \tag{8.14}$$

The transition rate, after orientational averaging, can again be written as

$$\langle \Gamma \rangle = N\mathscr{F}(\omega) I' B^{(2)}, \tag{8.15}$$

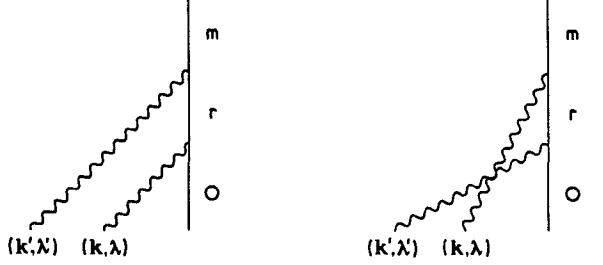

Figure 5. Time-ordered graphs for absorption of two photons from two beams.

where

$$B^{(2)}=\frac{1}{120\hbar^2 c\varepsilon_0}[A\alpha^{m0}_{\lambda\lambda}(\omega,\omega')\bar{\alpha}^{m0}_{\mu\mu}(\omega,\omega')+B\alpha^{m0}_{\lambda\mu}(\omega,\omega')\bar{\alpha}^{m0}_{\lambda\mu}(\omega,\omega')$$
$$+C\alpha^{m0}_{\lambda\mu}(\omega,\omega')\bar{\alpha}^{m0}_{\mu\lambda}(\omega,\omega')], \tag{8.16}$$

with

$$\left.\begin{aligned} A&=4|\mathbf{e}\cdot\mathbf{e}'|^2-1-|\mathbf{e}\cdot\bar{\mathbf{e}}'|^2,\\ B&=-|\mathbf{e}\cdot\mathbf{e}'|^2+4-|\mathbf{e}\cdot\bar{\mathbf{e}}'|^2,\\ C&=-|\mathbf{e}\cdot\mathbf{e}'|^2-1+4|\mathbf{e}\cdot\bar{\mathbf{e}}'|^2. \end{aligned}\right\} \tag{8.17}$$

In experiments using different propagation directions and polarizations, it is possible to obtain information about $\alpha^{m0}_{\lambda\mu}(\omega,\omega')$ (McClain 1974).

9. Static field-induced absorption

It is well known that a static field can perturb the energy levels of atoms and molecules, a process termed the Stark effect. Application of an electric field also produces a mixing of the eigenstates of the system as represented by (2.15). This generally results in a change in the selection rules for optical transitions, shown by the appearance of normally forbidden spectral features. A classic example is provided by the observation of fundamental vibration–rotation lines in the spectrum of molecular hydrogen.

Field-induced one-photon absorption of this kind was predicted by Condon (1932), who also drew attention to the analogy with Raman spectroscopy in the limit where the scattered photon is of zero frequency. The process may also be pictured as two-photon absorption with one photon of zero frequency, as shown by the time-ordered diagrams in figure 6. In these diagrams the horizontal line denotes the static field, which may be regarded as a zero-frequency field without propagation characteristics.

There are two routes to the rate expression for field-induced absorption. One involves time-dependent perturbation theory as in the case of two-photon absorption discussed in section 8. The alternative method, which leads to identical results, is to recast the rate equation for one-photon absorption in terms of base states dressed by a static electric displacement field **D** according to (2.15). For a system perturbed by the static field, (3.5) and (3.8) give the rate, for a system fixed in space:

$$\Gamma=\frac{\mathscr{I}(\omega)}{2\hbar^2\varepsilon_0}|\mathbf{e}^{(\lambda)}\cdot\boldsymbol{\mu}^{m'0'}|^2, \tag{9.1}$$

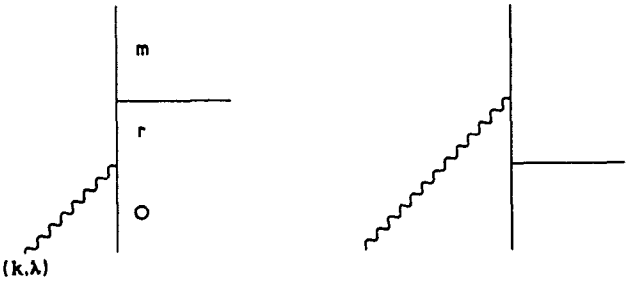

Figure 6. Graphs for field-induced one-photon absorption.

where the dressed states $|0'\rangle$ and $|m'\rangle$ are given by

$$|0'\rangle = |E_0\rangle + \varepsilon_0^{-1} \sum_{r \neq 0} (\boldsymbol{\mu}^{r0} \cdot \mathbf{D}) E_{r0}^{-1} |E_r\rangle + \ldots, \tag{9.2}$$

$$|m'\rangle = |E_m\rangle + \varepsilon_0^{-1} \sum_{r \neq m} (\boldsymbol{\mu}^{rm} \cdot \mathbf{D}) E_{rm}^{-1} |E_r\rangle + \ldots \quad . \tag{9.3}$$

For the interesting case where the transition $|m\rangle \leftarrow |0\rangle$ is electric-dipole-forbidden in the absence of the static field, we have $\boldsymbol{\mu}^{m0} = 0$, and the leading terms in the rate are

$$\Gamma = \frac{\mathscr{I}(\omega)}{2\hbar^2 \varepsilon_0^2} \left| \sum_{r \neq m} \frac{(\boldsymbol{\mu}^{mr} \cdot \mathbf{D})(\boldsymbol{\mu}^{r0} \cdot \mathbf{e}^{(\lambda)})}{E_{r0} - \hbar\omega} + \sum_{r \neq 0} \frac{(\boldsymbol{\mu}^{mr} \cdot \mathbf{e}^{(\lambda)})(\boldsymbol{\mu}^{r0} \cdot \mathbf{D})}{E_{r0}} \right|^2 . \tag{9.4}$$

The result is more conveniently expressed in terms of a molecular response tensor S_{ij} defined as

$$S_{ij}^{m0} = \sum_r \left(\frac{\mu_i^{mr} \mu_j^{r0}}{E_{r0} - \hbar\omega} + \frac{\mu_j^{mr} \mu_i^{r0}}{E_{r0}} \right). \tag{9.5}$$

Hence for a fluid sample the absorption rate is

$$\Gamma = \frac{\mathscr{I}(\omega)}{2\hbar^2 \varepsilon_0^2} \langle |S_{ij}^{m0} D_i e_j^{(\lambda)}|^2 \rangle. \tag{9.6}$$

First we consider the case where the sample molecules are non-polar, and not oriented by application of the static field. After performing the appropriate isotropic rotational average, we have for the rate

$$\Gamma = \frac{\mathscr{I}(\omega) D^2}{60\hbar^2 \varepsilon_0^2} [(3S_{\lambda\lambda}^{m0} S_{\mu\mu}^{m0} + 3S_{\lambda\mu}^{m0} S_{\mu\lambda}^{m0} - 2S_{\lambda\mu}^{m0} S_{\lambda\mu}^{m0}) \cos^2 \psi$$

$$- (S_{\lambda\lambda}^{m0} S_{\mu\mu}^{m0} + S_{\lambda\mu}^{m0} S_{\mu\lambda}^{m0} - 4S_{\lambda\mu}^{m0} S_{\lambda\mu}^{m0})], \tag{9.7}$$

where ψ is the angle between the direction of the static field and the electric polarization vector of the radiation. The result may be expressed in the form

$$\Gamma \propto 1 + \alpha \cos^2 \psi, \tag{9.8}$$

where

$$\alpha = \frac{3S_{\lambda\lambda}^{m0} S_{\mu\mu}^{m0} + 3S_{\lambda\mu}^{m0} S_{\mu\lambda}^{m0} - 2S_{\lambda\mu}^{m0} S_{\lambda\mu}^{m0}}{4S_{\lambda\mu}^{m0} S_{\lambda\mu}^{m0} - S_{\lambda\lambda}^{m0} S_{\mu\mu}^{m0} - S_{\lambda\mu}^{m0} S_{\mu\lambda}^{m0}}. \tag{9.9.}$$

Since ψ is experimentally controllable, a study of the ψ-dependence of each line in the field-induced spectrum enables a corresponding value of α to be determined. This can lead directly to a symmetry classification of each induced transition, in many cases giving an unambiguous result (Andrews and Sherborne 1984).

A separate issue is the change in intensity of dipole-allowed transitions in polar molecules on application of a static field. Here the result may be obtained from (9.1) by performing a Boltzmann-weighted orientational average taking into account the

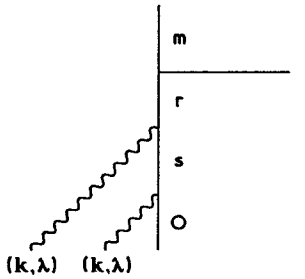

Figure 7. Typical graph for field-induced two-photon absorption.

preferential alignment of the molecules with the field (Andrews and Harlow 1984). The leading terms in this case are given by (Andrews and Sherborne 1986)

$$\Gamma = \frac{\mathscr{I}(\omega)}{12\hbar^2\varepsilon_0}\left[2|\boldsymbol{\mu}^{m0}|^2 + \left(\frac{3\coth\gamma}{\gamma} - \frac{3}{\gamma^2} - 1\right)(3\cos^2\psi - 1)(|\boldsymbol{\mu}^{m0}|^2 - 3|\boldsymbol{\mu}^{m0}\cdot\hat{\boldsymbol{\mu}}^{00}|^2)\right], \tag{9.10}$$

where

$$\gamma = \frac{\mu^{00}D}{\varepsilon_0 kT}. \tag{9.11}$$

and $\boldsymbol{\mu}^{00}$ is the permanent molecular dipole moment. Under normal experimental conditions $\gamma < 0{\cdot}1$, and the $\coth\gamma$ term is well approximated by a Taylor series. A comparison of (9.10) and (3.9) then shows that the field-induced change in the absorption rate is given approximately by

$$\Delta\Gamma = \frac{\mathscr{I}(\omega)\gamma^2}{180\hbar^2\varepsilon_0}(3\cos^2\psi - 1)(|\boldsymbol{\mu}^{m0}|^2 - 3|\boldsymbol{\mu}^{m0}\cdot\hat{\boldsymbol{\mu}}^{00}|^2). \tag{9.12}$$

The overall sign of the intensity change thus depends on both the experimentally variable angle ψ between the direction of the static field and the polarization direction of the radiation, and also on the molecule-fixed angle between the permanent and transition dipole moments.

Similar electro-optical effects arise in two-photon spectroscopy. Again the application of a static field can affect the appearance of a two-photon spectrum through two distinct mechanisms. One involves a nonlinear electro-optical channel in which the static field plays the role of a zero-frequency photon, as illustrated in the time-ordered diagram of figure 7. This mechanism results in the appearance of new lines allowed under three-photon selection rules in the two-photon spectrum. For example, transitions to excited states of B_{2u} symmetry in D_{6h} molecules, E_{3u} in $D_{\infty h}$ molecules, or A_{2u} in O_h species, which are rigorously forbidden under normal two-photon selection rules, all become allowed through the perturbing influence of the static field. The other mechanism, which is again specifically relevant to polar fluids, is associated with a partial molecular alignment produced by the applied field. The resultant anisotropy produces a relaxation of symmetry constraints on allowed two-photon transitions (Andrews *et al.* 1988).

10. Harmonic generation

Harmonic generation is a term used to describe the conversion of high-intensity laser radiation into output radiation with a frequency ω' equal to a multiple m times the input frequency ω. It depends on incident fields strong enough to excite the nonlinear

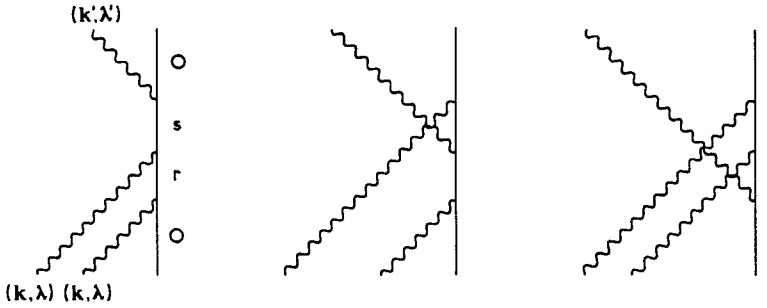

Figure 8. Graphs for second-harmonic generation.

response of a molecule. Familar light-scattering processes, such as Rayleigh scattering, depend only on the linear part of the molecular response. In quantum electrodynamical terms the process comprises the annihilation of m laser photons and the creation of an mth-harmonic photon, the state of the conversion medium remaining unchanged overall. One of the distinctive features is that such processes generally entail constructive interference between signals from different molecules in the sample, and are therefore termed *coherent*. The result is that harmonic generation is associated with conversion efficiencies that are remarkable for multiphoton processes. Consequently harmonic generation is widely used for the upward frequency conversion of laser radiation.

The quantum electrodynamical representation of harmonic generation is best illustrated by reference to the most familiar example, second-harmonic generation (SHG), often referred to as frequency doubling. Two pump photons $(\mathbf{k}, \lambda)$ are destroyed and one second-harmonic photon $(\mathbf{k}', \lambda')$ created in each interaction; the appropriate time-ordered diagrams are shown in figure 8. The corresponding matrix element for a molecule ζ located at $\mathbf{R}_\zeta$ is given by

$$M_{\mathrm{fi}}(\zeta) = -\mathrm{i}\left(\frac{\hbar c}{2\varepsilon_0 V}\right)^{3/2} (k^2 k')^{1/2}[n(n-1)]^{1/2}\beta_{ijk}(\zeta)\bar{e}'_i e_j e_k \exp[\mathrm{i}(2\mathbf{k}-\mathbf{k}')\cdot\mathbf{R}_\zeta], \qquad (10.1)$$

where β_{ijk} is the hyperpolarizability tensor given by

$$\begin{aligned}\beta_{ijk} = \frac{1}{2}\sum_{r,s}\Bigg[&\frac{\mu_i^{0s}\mu_j^{sr}\mu_k^{r0}}{(E_{s0}-2\hbar\omega)(E_{r0}-\hbar\omega)} + \frac{\mu_j^{0s}\mu_i^{sr}\mu_k^{r0}}{(E_{s0}+\hbar\omega)(E_{r0}-\hbar\omega)} \\ &+ \frac{\mu_j^{0s}\mu_k^{sr}\mu_i^{r0}}{(E_{s0}+\hbar\omega)(E_{r0}+2\hbar\omega)} + \frac{\mu_i^{0s}\mu_k^{sr}\mu_j^{r0}}{(E_{s0}-2\hbar\omega)(E_{r0}-\hbar\omega)} \\ &+ \frac{\mu_k^{0s}\mu_i^{sr}\mu_j^{r0}}{(E_{s0}+\hbar\omega)(E_{r0}-\hbar\omega)} + \frac{\mu_k^{0s}\mu_j^{sr}\mu_i^{r0}}{(E_{s0}+\hbar\omega)(E_{r0}+2\hbar\omega)}\Bigg].\end{aligned} \qquad (10.2)$$

In (10.1) n is the number of pump photons in the quantization volume V, and $\mathbf{e}$ and $\mathbf{e}'$ are the polarization vectors for the pump and second-harmonic photons respectively. It is essential to retain the phase factor in (10.1) since it is responsible for determining coherent response.

In general, the collective signal from a molecular ensemble is given by the Fermi rule

$$\Gamma = \frac{2\pi}{\hbar}\left|\sum_{\zeta} M_{\mathrm{fi}}(\zeta)\right|^2 \rho, \tag{10.3}$$

where the summation is over all molecules within the interaction volume; ρ is the density of radiation states in the energy region of the harmonic frequency $\omega' = 2\omega$. When all molecules are of the same chemical species, differences between the individual matrix elements $M_{\mathrm{fi}}(\zeta)$ result only from the differing displacements and orientations within the sample. For a fluid it is helpful to rewrite (10.3) as a sum of diagonal (one-centre) and off-diagonal (correlation) terms:

$$\Gamma = \frac{2\pi}{\hbar}\sum_{\zeta}\langle|M_{\mathrm{fi}}|^2\rangle\rho + \frac{2\pi}{\hbar}\sum_{\zeta'\neq\zeta}\langle M_{\mathrm{fi}}(\zeta)\rangle\langle\bar{M}_{\mathrm{fi}}(\zeta')\rangle\rho, \tag{10.4}$$

where the angular brackets denote the rotational average.

In evaluating the first term of (10.4), the position-dependent phase factors disappear, and orientational differences between contributions from different molecules vanish on rotational averaging. This term therefore gives an overall rate contribution that is directly proportional to the number of scatterers N, and thus represents the *incoherent* signal:

$$\Gamma_{\mathrm{incoh}} = \frac{2\pi N}{\hbar}\langle|M_{\mathrm{fi}}|^2\rangle\rho. \tag{10.5}$$

The second term of (10.4), however, involves a product of phase factors associated with different molecules, and represents a *coherent* contribution:

$$\Gamma_{\mathrm{coh}} = \frac{2\pi}{\hbar}\sum_{\zeta\neq\zeta'}|\langle M_{\mathrm{fi}}\rangle|^2\rho\exp\left[\mathrm{i}(2\mathbf{k}-\mathbf{k}')\cdot(\mathbf{R}_{\zeta}-\mathbf{R}_{\zeta'})\right]. \tag{10.6}$$

In the general case summation leads to complete cancellation of the various cross-terms through destructive interference in the phase factors. The important exception is harmonic generation, where $\mathbf{k}' = 2\mathbf{k}$, since then the phase factors disappear and the interference between the signals from different molecules is constructive. This corresponds to forward phase-matched emission of the second harmonic. The essentially quadratic dependence of the emission rate on N means that for high intensity the coherent contribution far outweighs the incoherent, and the rate of harmonic conversion is effectively given by

$$\Gamma_{\mathrm{coh}} = \frac{2\pi N^2}{\hbar}|\langle M_{\mathrm{fi}}\rangle|^2\rho. \tag{10.7}$$

This result can be re-expressed in terms of physically measured optical quantities to give the following expression for the radiant intensity I^{SHG} of second-harmonic generation:

$$I^{\mathrm{SHG}} = \frac{k^4}{\pi^2\varepsilon_0^2} I^2 g^{(2)} N^2 |\langle\beta_{ijk}\bar{e}'_i e_j e_k\rangle|^2, \tag{10.8}$$

where I is the irradiance of the pump laser and $g^{(2)}$ its degree of second-order coherence (8.13).

A number of significant features emerge from an examination of the structure of (10.8). First, it is clear that, since the hyperpolarizability itself vanishes in any

centrosymmetric molecule, SHG cannot be supported in any medium composed of molecules of this type. This simply reflects the fact that an odd number of electric dipole transitions cannot connect two molecular states of the same parity, as the initial and final state for SHG necessarily are. The second implication is that SHG cannot occur within any fluid medium that has *macroscopic* isotropy. The proof of this is less straightforward, and is somewhat obscured in the classical description of harmonic generation. The result essentially arises from the fact that the isotropic parts of both the hyperpolarizability tensor and the third-rank polarization tensor $\bar{e}'_i e_j e_k$ vanish. Similar remarks apply even when higher-order multipolar contributions are considered. Consequently the rotational average in (10.8) is zero, and coherent harmonic emission is thus forbidden in isotropic fluids (Andrews and Blake 1988). The result has interesting practical implications, since it facilitates the use of SHG as a surface-specific probe. For this reason harmonic generation has become an important tool for studying the chemistry of interfaces (Shen 1984).

Although SHG is normally forbidden in isotropic media, the application of a static electric field can remove the forbidden character of the process by two distinct mechanisms. These relate closely to the two transition routes for electric-field-induced absorption discussed in section 9. In the first mechanism the static electric field induces an electro-optical contribution to the harmonic signal at the molecular level. This contribution is calculated using fourth-order perturbation theory with the aid of time-ordered graphs of the kind shown in figure 9. By this mechanism, SHG becomes allowed both in centrosymmetric crystals and in fluids. The second mechanism applies to fluids consisting of polar (and thus necessarily non-centrosymmetric) molecules. Here the electric field removes bulk isotropy by inducing a degree of molecular alignment, governed under equilibrium conditions by the Boltzmann distribution law. In contrast with the result (10.8), application of a static field thus produces a radiant second-harmonic intensity

$$I^{\mathrm{SHG}} = \frac{k^4}{\pi^2 \varepsilon_0^2} I^2 g^{(2)} N^2 |\langle \beta_{ijk} \bar{e}'_i e_j e_k + \varepsilon_0^{-1} \chi_{ijkl} \bar{e}'_i e_j e_k D_l \rangle|^2. \tag{10.9}$$

Here the correction term involving the fourth-rank tensor χ_{ijkl} represents the local electro-optical interaction, and the angular brackets now represent an orientational average weighted by the Boltzmann factor γ, defined by (9.11), for the energy of dipole coupling with the local electric field. The full structure of the result including the form of the tensor χ_{ijkl} is given elsewhere (Lam and Thirunamachandran 1982, Andrews and Sherborne 1986).

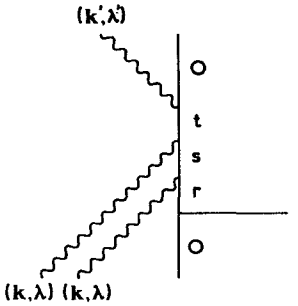

Figure 9. Typical graph for field-induced second-harmonic generation.

Here it is appropriate to draw out a few salient features of the dependence of SHG intensity on experimental variables. These are principally the laser polarization, electric field strength and temperature. Under normal low-field conditions where $\gamma \ll 1$, the harmonic intensity may be expressed by the following leading terms in a Taylor series:

$$I^{\mathrm{SHG}} = \frac{k^4}{225\pi^2\varepsilon_0^4} I^2 g^{(2)} D^2 N^2 \left| (3p_1 - p_2)\left(\chi_{\lambda\lambda\mu\mu} + \frac{1}{kT}\beta_{\lambda\lambda\mu}\mu_\mu^{00}\right) + (2p_2 - p_1)\left(\chi_{\lambda\mu\mu\lambda} + \frac{1}{kT}\beta_{\lambda\mu\mu}\mu_\lambda^{00}\right)\right|^2. \quad (10.10)$$

Here p_1 and p_2 are polarization parameters given by

$$p_1 = (\bar{\mathbf{e}}' \cdot \mathbf{e})(\mathbf{e} \cdot \hat{\mathbf{D}}), \quad (10.11)$$

$$p_2 = (\bar{\mathbf{e}}' \cdot \hat{\mathbf{D}})(\mathbf{e} \cdot \mathbf{e}). \quad (10.12)$$

Clearly the harmonic signal disappears entirely when the static field is applied parallel to the pump beam; this remains true even when all higher orders in the Taylor series are considered. It is therefore normal practice to apply the field perpendicularly, and the conversion efficiency can be maximized with a spatially periodic field (Shelton and Buckingham 1982). Selective temperature measurements in different geometries allow direct evaluation of the parameters $\chi_{\lambda\lambda\mu\mu}$, $\chi_{\lambda\mu\mu\lambda}$, $\beta_{\lambda\mu\mu}\mu_\lambda$ and $\beta_{\lambda\lambda\mu}\mu_\mu$. Such parameters provide significant information on molecular electronic properties such as the extent of delocalization in extended conjugated species (Chemla and Zyss 1987).

11. Resonance interaction

In a system of two identical molecules A and B, with excited states $|E_m^{\mathrm{A}}\rangle$ and $|E_m^{\mathrm{B}}\rangle$, the product states $|E_m^{\mathrm{A}}, E_0^{\mathrm{B}}\rangle$ and $|E_0^{\mathrm{A}}, E_m^{\mathrm{B}}\rangle$ are equal in energy; they are interconverted by excitation exchange. They may be used to form stationary states, which are

$$2^{-1/2}(|E_m^{\mathrm{A}}, E_0^{\mathrm{B}}\rangle \pm |E_0^{\mathrm{A}}, E_m^{\mathrm{B}}\rangle), \quad (11.1)$$

with an energy splitting equal to the real part of

$$2\langle E_m^{\mathrm{B}}, E_0^{\mathrm{A}}|H_{\mathrm{int}}|E_m^{\mathrm{A}}, E_0^{\mathrm{B}}\rangle, \quad (11.2)$$

H_{int} being the intermolecular coupling operator. The familiar exciton splitting measured in molecular crystals is a sum of (11.2) over a lattice of identical molecules (Craig and Walmsley 1967). If time is too short to reach a stationary state then $|E_m^{\mathrm{A}}, E_0^{\mathrm{B}}\rangle$ is non-stationary and may decay either by transfer of energy to its partner or by photon emission (fluorescence), leaving both molecules in their ground states $|E_0^{\mathrm{A}}, E_0^{\mathrm{B}}\rangle$. In the former case the rate of energy transfer (Förster rate) may be characterized by a lifetime when there are many identical systems into which $|E_m^{\mathrm{A}}\rangle$ may transfer energy and when the corresponding energy levels are spread over a range of energy by solvent perturbation. There are also cases that are intermediate between stationary states and exponentially decaying states.

This simple description can be framed accurately in QED, and shown to be related in all cases to the primitive processes of photon absorption and emission, not only in the fluorescence limit. We noted earlier that in the multipolar formalism the coupling between two neutral molecules is mediated by transverse photons. The coupling matrix element can be calculated with the aid of time-ordered diagrams. If A is the molecule initially excited then the time-ordered diagram (*a*) in figure 10 contributes a term

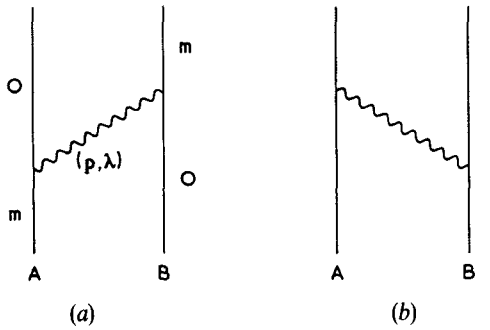

Figure 10. Graphs for resonance coupling.

corresponding to emission from A followed by absorption by B. Diagram (*b*) applies to the time sequence in which the first event is virtual emission by B and excitation of it to $|E_m^B\rangle$. We note here an important difference from virtual processes in one-centre cases such as two-photon absorption (section 8). In applying the uncertainty relation $\Delta E\,\Delta t \sim \frac{1}{2}\hbar$ in a one-centre example, Δt is the time interval for the excitation of the atom or molecule. This is a time so short that ΔE becomes much larger than the transition energies, and all virtual processes are feasible. For two-centre problems the time Δt within which the photon energy is transferred is determined in a different way, namely by the photon transit time from A to B at the speed of light. At an A–B spacing of 1 nm we find $\Delta E \sim 2{\cdot}4 \times 10^{16}$ Hz, or $8 \times 10^5\ \mathrm{cm}^{-1}$. Energies far in excess of E_{m0} can thus be borrowed from the vacuum for the similar process in diagram (*b*); even at 10 nm ($\Delta E \sim 8 \times 10^4\ \mathrm{cm}^{-1}$) the same is true. However, at about 40 nm (*b*) could not contribute. The photons in diagram (*b*), and the transitions at the vertices, are possible through this energy borrowing and are *virtual*. We now go back to diagram (*a*), noting that the same argument applies. The contribution is a sum over all frequencies, real and virtual, but here there is the difference that one frequency is exactly resonant with the transition frequency $E_{m0}/\hbar$. The two diagrams in figure 10 apply to the case where A is initially excited and they describe energy transfer from A to B. The matrix element M_{fi} for this process is complex, and the transfer rate is found from the Fermi rule

$$\Gamma = \frac{2\pi}{\hbar}|M_{\mathrm{fi}}|^2\rho, \tag{11.3}$$

with ρ the density of states, namely the density of radiation field states in the vicinity of the transition energy E_{m0}. The transfer matrix element is given by (11.4) (Power and Thirunamachandran 1983, Andrews and Sherborne 1987, Craig and Thirunamachandran 1989):

$$M_{\mathrm{fi}} = \frac{1}{4\pi\varepsilon_0 R^3}\mu_i^{0m}(\mathrm{A})\mu_j^{m0}(\mathrm{B})[\beta_{ij}(1-\mathrm{i}kR)-\alpha_{ij}k^2R^2]\exp(\mathrm{i}kR), \tag{11.4}$$

where

$$\beta_{ij} = \delta_{ij} - 3\hat{R}_i\hat{R}_j, \tag{11.5}$$

$$\alpha_{ij} = \delta_{ij} - \hat{R}_i\hat{R}_j. \tag{11.6}$$

Here μ^{m0} is the dipole transition moment connecting the levels m and 0, k is the wavenumber and R is the separation distance. The significance of β_{ij} and α_{ij} may be seen as follows. In the small-R limit (the near-zone limit) the expression (11.4) reduces to

$$\frac{1}{4\pi\varepsilon_0 R^3}\mu_i^{0m}(\mathrm{A})\mu_j^{m0}(\mathrm{B})\beta_{ij}. \tag{11.7}$$

We recognize this as the expression for the electrostatic dipole–dipole interaction energy; β_{ij} describes a coupling of both longitudinal and transverse components. At large enough R (the far zone) the matrix element (11.4) becomes

$$-\frac{k^2}{4\pi\varepsilon_0 R}\mu_i^{0m}(\mathrm{A})\mu_j^{m0}(\mathrm{B})\alpha_{ij}\exp(ikR). \tag{11.8}$$

We see that the components of μ^{m0} along the molecular join make no contribution to the coupling energy. The dyadic α_{ij} is purely transverse. The interaction (11.4) is due to the electric vector at A as a radiation source acting on the transition dipole at B.

The rate of energy transfer found from the Fermi rule (11.3) together with (11.4) for the matrix element is

$$\Gamma(\mathrm{A}\rightarrow\mathrm{B})=\frac{|\mu^{m0}(\mathrm{A})|^2|\mu^{0m}(\mathrm{B})|^2}{36\pi\varepsilon_0^2\hbar R^6}(3+k^2R^2+k^4R^4)\rho. \tag{11.9}$$

The conditions of validity of this expression are restricted. It applies over times τ for which $\hbar/|M_{\mathrm{fi}}|\ll\tau\ll\Gamma^{-1}$. The second inequality implies that the interval must be limited to the early stages of decay over times much less than the decay lifetime Γ^{-1}. The first inequality implies that τ must be much greater than the characteristic period of excitation exchange between the resonating pair, as determined by the coupling between them. That is, the decaying system must be quasi-stationary over the period of observation, and must decay only by a small fraction of its initial population. As an example, let us suppose that two molecules in resonance have a coupling matrix element of energy equivalent to 100 cm^{-1}. The characteristic period of energy exchange is 3×10^{-13} s. If the pair excitation is decaying only by fluorescence then the lifetime of about 10^{-9} s calculated by the Fermi rule is valid over, say, the first 10% of decay. However, where the matrix element is very small, say $10^{-3}\,\mathrm{cm}^{-1}$, we can say that the excitation transfer period from A to B is slow compared with the de-excitation of A by fluorescence. In that case the Fermi rule applies to the decay of excited A, not the decay of the resonating pair.

There are other interesting features of resonance transfer, discussed in detail elsewhere (Craig 1989, Craig and Thirunamachandran 1989). We note two only. The first is that the limiting long-range rate from (11.9) is

$$\Gamma_{\mathrm{lim}}=\frac{|\mu^{m0}|^4k^4\rho}{36\pi\varepsilon_0^2\hbar R^2}, \tag{11.10}$$

where ρ is the density of states of the radiation field. From its derivation we can assert that this is the rate of irreversible molecule-to-molecule excitation transfer driven by intermolecular coupling. It is at first surprising to find (Andrews 1989a) that this is exactly equal to a rate found by calculating the fluorescence emission by A, and then finding the absorption of the emitted light by B, viewed as two uncorrelated processes with no direct A–B interaction.

Inasmuch as in the wave zone the transfer rate for the one-to-one interaction of identical systems is the same as the rate for independent processes of spontaneous emission and absorption, we see that the nature and properties of B are not relevant to the emission rate by A, although they determine the characteristics of the subsequent absorption. Equally, the presence of other B molecules does not change the emission rate, as is obvious. Thus in the wave zone the only states that contribute to the density ρ are states of the radiation.

On the other hand, in the complete Fermi expression (11.9) other final states contribute in some cases. Whereas in the wave zone the decay rate (11.10) is independent of the number of absorbers, this is not true of interaction at short range. If we have N absorbers B, supposed not to be coupled to each other, then $|E_m^{\mathrm{A}}\rangle$ is coupled for energy transfer to the N degenerate states

$$\left.\begin{array}{l} |E_m^{\mathrm{B}1}\rangle|E_0^{\mathrm{B}2}\rangle\ldots|E_0^{\mathrm{B}N}\rangle \\ |E_0^{\mathrm{B}1}\rangle|E_m^{\mathrm{B}2}\rangle\ldots|E_0^{\mathrm{B}N}\rangle \\ \quad\vdots \\ |E_0^{\mathrm{B}1}\rangle|E_0^{\mathrm{B}2}\rangle\ldots|E_m^{\mathrm{B}N}\rangle \end{array}\right\} \tag{11.11}$$

where BN denotes the Nth molecule of species B. The total decay rate is made up of terms for N pairwise one-to-one interactions. In the framework of (11.9) this is dealt with in the definition of the density of states. If the N molecules of B are in solution then coupling to solvent molecules will cause a range of energy displacements, and an ensemble molecular density ρ_{mol} can be defined. The argument can be extended to transfer from A to non-identical systems B, where the resonance condition applies to the pure electronic excited state of A and vibronic sublevels of an excited state of B. Both cases are examples of Förster transfer. We note the important point that in this case the coupling does not depend on the total $|\boldsymbol{\mu}^{m0}(\mathrm{B})|^2$ but only on the fraction of it belonging to the sublevels of B that overlap (within the linewidth) with the single level of A.

Secondly, there is the connection expected from the correspondence principle between the decay rate of an excited system calculated by quantum mechanics and the classical rate of energy loss from an oscillating dipole in an antenna. We readily find the power loss through a spherical surface surrounding an excited molecule to be

$$P_{\mathrm{spont}} = \frac{ck^4}{3\pi\varepsilon_0}|\boldsymbol{\mu}|^2, \tag{11.12}$$

which is the product of the Einstein A-coefficient and the energy quantum $\hbar ck$. The classically calculated power loss from a dipole antenna with moment $\mathbf{p}$, via the Poynting vector

$$\mathbf{S} = \varepsilon_0 c^2(\mathbf{E}\times\mathbf{B}), \tag{11.13}$$

is

$$P_{\mathrm{rad}} = \frac{ck^4}{12\pi\varepsilon_0}|\mathbf{p}|^2, \tag{11.14}$$

where

$$\mathbf{P} = \int \mathbf{r}'\rho(\mathbf{r}')\,\mathrm{d}^3\mathbf{r}', \tag{11.15}$$

$\rho(\mathbf{r}')$ being the charge density. The rates (11.12) and (11.14) are equal if the classical $\mathbf{p}$ is twice as large as the dipole matrix element $\boldsymbol{\mu}$. This relation can be shown to hold for the harmonic oscillator.

Finally, for a radiating dipole the Poynting vector shows an r^{-2} dependence. That this must be so can be inferred from local conservation of energy (Lorrain and Corson 1970, p. 604), since the energy flow through a spherical surface must be independent of the radius. The inverse-square dependence is in accord with the limiting transfer rate (11.10).

12. Resonance interaction relayed through a third molecule

In many practical cases, such as energy transfer in a fluid medium, the two identical molecules A and B are in a solvent consisting of molecules C or are in solution together with other solutes. In a macroscopic description of the resonance coupling of A and B the effect of a solvent is taken care of through the use of the solvent permittivity ε in place of the vacuum permittivity ε_0 in the near-zone dipole coupling (11.7). Thus we have

$$\frac{1}{4\pi\varepsilon R^3}\mu_i^{m0}(\mathrm{A})\mu_j^{0m}(\mathrm{B})\beta_{ij}. \tag{12.1}$$

The problem discussed in this section is the connection between the macroscopic model, namely that of coupled molecules immersed in a dielectric medium, and the microscopic theory in which interactions between A and B are relayed through the individual molecules C that make up the medium. From the latter point of view the effect of the medium is an average over a large number of three-, four- and many-body terms A–C–B, A–C–C–B and A–$(C)_n$–B. Every molecule is individually included, and each interaction has the vacuum permittivity ε_0. At low densities, in the macroscopic picture, ε exceeds ε_0 by a very small quantity only. In the microscopic picture the direct interaction (12.1) is accompanied by interactions through C, as in A–C–B, which we now consider.

In QED the time-ordered diagrams for a three-body resonance interaction process are illustrated by a typical graph (*a*) in figure 11. In this graph A is initially in an excited state $|E_m^{\mathrm{A}}\rangle$. Photon emission excites C to one of its states $|E_n^{\mathrm{C}}\rangle$, and in a further step B is left in excited state $|E_m^{\mathrm{B}}\rangle$. Overall, excitation has been transferred from A to B. The states of C that enter as intermediate states are summed over, and can be shown to appear

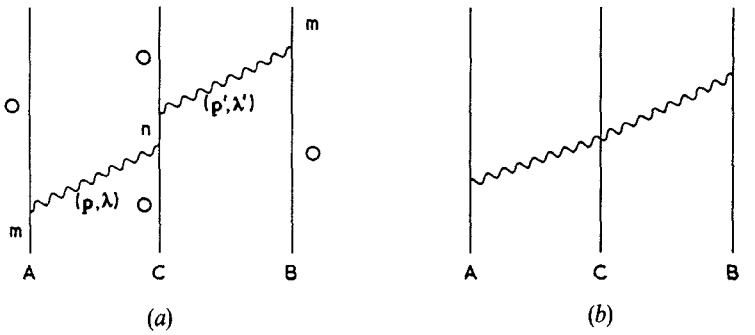

(*a*) (*b*)

Figure 11. (*a*) Typical graph for resonance coupling relayed through a third molecule. (*b*) Typical graph using effective two-photon interaction vertex.

exactly as in the dynamic polarizability (12.4). We are thus able to replace the sets of diagrams referring to various states n by a small number like diagram (*b*), in which the interaction vertex is

$$-\varepsilon_0^{-2}\alpha_{jk}(\mathrm{C};k)d_j(\mathbf{p})d_k(\mathbf{k}). \tag{12.2}$$

In the near zone the contribution to the transfer matrix element is

$$M_{\mathrm{fi}}\approx\frac{1}{(4\pi\varepsilon_0)^2R^3R'^3}\mu_i^{m0}(\mathrm{A})\mu_j^{0m}(\mathrm{B})\alpha_{kl}(\mathrm{C};k)(\delta_{il}-3\hat{R}_i\hat{R}_l)(\delta_{jk}-3\hat{R}'_j\hat{R}'_k), \tag{12.3}$$

where R and R' are the distances A–C and C–B; $\alpha_{kl}(\mathrm{C};k)$ is a component of the dynamic polarizability of C at frequency ck,

$$\alpha_{kl}(k)=\sum_r\left(\frac{\mu_k^{0r}\mu_l^{r0}}{E_{r0}-\hbar ck}+\frac{\mu_l^{0r}\mu_k^{r0}}{E_{r0}+\hbar ck}\right). \tag{12.4}$$

Now, since in replacing the vacuum energy for direct interaction by that for the medium we get an interaction reduced in the ratio $\varepsilon_0/\varepsilon$, we must verify that inclusion of the microscopic relayed interaction also causes a reduction, when an average is taken over all orientations and positions of C. This can be seen as follows. In the three-body problem the molecular states are $|E_m^{\mathrm{A}}, E_0^{\mathrm{B}}, E_0^{\mathrm{C}}\rangle$, $|E_0^{\mathrm{A}}, E_m^{\mathrm{B}}, E_0^{\mathrm{C}}\rangle$ and $|E_0^{\mathrm{A}}, E_0^{\mathrm{B}}, E_n^{\mathrm{C}}\rangle$, the latter being taken for all excited states n. The first two are the initial and final states for the direct resonance coupling. If for purposes of illustration we take H_{int} to be the near-zone part of the dipole–dipole coupling operator, and omit the radiation field states throughout, we have for the first-order corrected three-molecule state (with B excited)

$$c_0|E_0^{\mathrm{A}}, E_m^{\mathrm{B}}, E_0^{\mathrm{C}}\rangle+\sum_n\frac{\langle E_0^{\mathrm{A}}, E_0^{\mathrm{B}}, E_n^{\mathrm{C}}|H_{\mathrm{int}}|E_0^{\mathrm{A}}, E_m^{\mathrm{B}}, E_0^{\mathrm{C}}\rangle}{E_m-E_n}|E_0^{\mathrm{A}}, E_0^{\mathrm{B}}, E_n^{\mathrm{C}}\rangle$$

$$+\sum_n\frac{\langle E_m^{\mathrm{A}}, E_m^{\mathrm{B}}, E_n^{\mathrm{C}}|H_{\mathrm{int}}|E_0^{\mathrm{A}}, E_m^{\mathrm{B}}, E_0^{\mathrm{C}}\rangle}{E_m+E_n}|E_m^{\mathrm{A}}, E_m^{\mathrm{B}}, E_n^{\mathrm{C}}\rangle. \tag{12.5}$$

The normalization condition is

$$c_0^2+\sum_n c_n'^2+\sum_n c_n''^2=1. \tag{12.6}$$

c_n' is the n-dependent perturbation coefficient in the second term of (12.5), and c_n'' is the corresponding coefficient in the third. The total resonance interaction is found by coupling (12.5) with $|E_m^{\mathrm{A}}, E_0^{\mathrm{B}}, E_0^{\mathrm{C}}\rangle$. The leading term is the direct coupling times the coefficient c_0^2. As the number of C molecules taking part in the interaction increases, so does the total contribution by indirect terms; then from the normalization condition (12.6) c_0^2 must decrease. The direct A–B term thus becomes decreasingly important compared with the indirect A–C–B terms. As the direct A–B term is progressively *replaced* by A–C–B and since the averaged values of the latter are then smaller, the net result is a reduction of the total. The outcome in the high-concentration limit can be seen in principle: the direct A–B part is entirely swamped (actually entirely replaced) by the indirect part. In practice increasing the number of C molecules involves dominance by A–$(\mathrm{C})_n$–B terms and we cannot make a calculation valid at high concentration of C by perturbation theory. However, it is qualitatively apparent that the macroscopic and microscopic viewpoints can be harmonized.

13. The dispersion interaction

In practical applications to chemical systems, and also historically, this is the most important form of coupling between molecules. Before quantum mechanics, the dispersion interaction was understood in terms of charge fluctuation in one molecule causing a response in the other, with a resultant energy having R^{-6} dependence on the intermolecular separation R. One had the model that the dipole $\mu_i(\mathrm{A})$ from fluctuation in A, through its electric field component E_j at B,

$$E_j = \frac{\mu_i(\mathrm{A})}{4\pi\varepsilon_0 R^3}\beta_{ij}, \tag{13.1}$$

induced a moment in B proportional to the polarizability,

$$\mu_k(\mathrm{B}) = \alpha_{jk}(\mathrm{B})E_j = -\frac{\alpha_{jk}(\mathrm{B})\mu_i(\mathrm{A})}{4\pi\varepsilon_0 R^3}\beta_{ij}, \tag{13.2}$$

with an associated energy shift

$$\Delta E = -\frac{\mu_i(\mathrm{A})\mu_l(\mathrm{A})}{16\pi^2\varepsilon_0^2 R^6}\alpha_{jk}(\mathrm{B})\beta_{ij}\beta_{kl}. \tag{13.3}$$

In molecular quantum mechanics the classical fluctuations appear as virtual transitions in the familiar manner, and the well known expression for the dispersion energy, after rotational averaging, is

$$\Delta E = -\frac{1}{24\pi^2\varepsilon_0^2 R^6}\sum_{r,s}\frac{|\mu^{r0}(\mathrm{A})|^2|\mu^{s0}(\mathrm{B})|^2}{E^{\mathrm{A}}_{r0}+E^{\mathrm{B}}_{s0}}. \tag{13.4}$$

The classical expression (13.3) and the semi-classical (13.4) owe their R^{-6} dependence to electrostatic (Coulombic) interactions valid at short distances; they reflect the Coulomb dipole–dipole R^{-3} distance law taken to second order. Although for a long time it had been understood that the law must be modified at distances too great for the propagation of electric fields to be considered instantaneous, the first correct theory was that of Casimir and Polder (1948), who, using the minimal-coupling Hamiltonian and taking complete account of retardation, obtained an expression for the dispersion energy valid for all separations outside the overlap region. In particular they showed that for large R the inverse sixth-power dependence on distance, predicted by the London theory, was replaced by the inverse seventh-power dependence

$$\Delta E = -\frac{23\hbar c}{64\pi^3\varepsilon_0^2}\frac{\alpha(\mathrm{A})\alpha(\mathrm{B})}{R^7}. \tag{13.5}$$

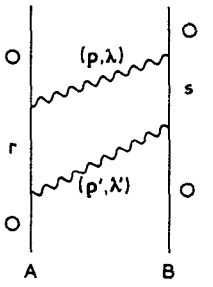

Figure 12. Typical graph for dispersion interactions.

The R^{-7} dependence was later confirmed experimentally by Tabor and Winterton (1969). The Casimir–Polder result was subsequently recovered using the multipolar form of quantum electrodynamics (Power and Zienau 1957, Craig and Power 1969).

With the multipolar Hamiltonian, interactions between neutral molecules are mediated by exchange of virtual photons. Energy shifts are manifestations of the exchange and may be calculated using conventional perturbation theory and time-ordered graphs. The leading contribution to the dispersion energy is of fourth order in $H_{\rm int}$:

$$\Delta E = -\sum_{I,II,III} \frac{\langle 0|H_{\rm int}|III\rangle\langle III|H_{\rm int}|II\rangle\langle II|H_{\rm int}|I\rangle\langle I|H_{\rm int}|0\rangle}{(E_I-E_0)(E_{II}-E_0)(E_{III}-E_0)} + \sum_{I,II} \frac{\langle 0|H_{\rm int}|II\rangle\langle II|H_{\rm int}|0\rangle\langle 0|H_{\rm int}|I\rangle\langle I|H_{\rm int}|0\rangle}{(E_I-E_0)^2(E_{II}-E_0)}. \tag{13.6}$$

The second term in (13.6) arises from wavefunction renormalization. It does not contribute to coupling between non-polar molecules. In (13.6) the ket $|0\rangle$ is the unperturbed ground state of the system, namely $|E_0^{\rm A}, E_0^{\rm B}; 0\rangle$. The intermediate states are of four types, depending on whether neither, one or both molecules are excited and whether zero, one or two photons are present. Twelve diagrams contribute to the dispersion interaction between non-polar molecules. A typical diagram is shown in figure 12. The corresponding intermediate states are

$$\left.\begin{aligned} |I\rangle &= |E_r^{\rm A}, E_0^{\rm B}; 1(\mathbf{p}', \lambda')\rangle, \\ |II\rangle &= |E_r^{\rm A}, E_s^{\rm B}; 0\rangle, \\ |III\rangle &= |E_0^{\rm A}, E_s^{\rm B}; 1(\mathbf{p}, \lambda)\rangle. \end{aligned}\right\} \tag{13.7}$$

In the electric dipole approximation for $H_{\rm int}$ we find for the energy shift

$$\Delta E = -\sum_{\substack{\mathbf{p},\mathbf{p}'\\ r,s}} \frac{\hbar cp}{2\varepsilon_0 V}\frac{\hbar cp'}{2\varepsilon_0 V}(\delta_{ik}-\hat{p}_i\hat{p}_k)(\delta_{jl}-\hat{p}'_j\hat{p}'_l)\mu_i^{0r}\mu_j^{r0}\mu_k^{0s}\mu_l^{s0} \times \exp[\mathrm{i}(\mathbf{p}+\mathbf{p}')\cdot\mathbf{R}]\sum_{a=\mathrm{i}}^{\mathrm{xii}} D_a^{-1}, \tag{13.7}$$

where D_a is one of the denominators for the twelve diagrams. The denominator sum is found to be (Craig and Thirunamachandran 1984)

$$\sum_{a=\mathrm{i}}^{\mathrm{xii}} D_a^{-1} = \frac{4\hbar^{-3}c^{-3}(k_{r0}+k_{s0}+p)}{(k_{r0}+k_{s0})(k_{r0}+p)(k_{s0}+p)}\left(\frac{1}{p+p'}-\frac{1}{p-p'}\right). \tag{13.8}$$

Virtual-photon summation is straightforward and we obtain the full Casimir–Polder result for a pair of freely rotating molecules:

$$\Delta E = -\frac{1}{36\pi^3\varepsilon_0^2\hbar cR^2}\sum_{r,s}|\boldsymbol{\mu}^{r0}|^2|\boldsymbol{\mu}^{s0}|^2 \times \int_0^\infty \frac{k_{r0}k_{s0}u^4\exp(-2uR)}{(k_{r0}^2+u^2)(k_{s0}^2+u^2)}\left(1+\frac{2}{uR}+\frac{5}{u^2R^2}+\frac{6}{u^3R^3}+\frac{3}{u^4R^4}\right)\mathrm{d}u. \tag{13.9}$$

It has already been noted that virtual transitions are made with energy 'borrowed' from the electromagnetic vacuum subject to the energy–time uncertainty relation $\Delta E\,\Delta t \gtrsim \frac{1}{2}\hbar$; Δt is the time taken for a signal to propagate from one molecule to the

other. Large separation distances thus correspond to small values of energy that can be borrowed from the vacuum. In the far-zone limit, u^2 in the energy denominators of (13.9) can be neglected in comparison with k_{r0} and k_{s0}. The u-integral then follows immediately and we obtain the R^{-7} result (13.5). In the near zone, $kR \ll 1$, the exponential in (13.9) can be set to unity and it is sufficient to retain the $(uR)^{-4}$ term. Thus

$$\Delta E = -\frac{1}{12\pi^3\varepsilon_0^2\hbar c R^6}\sum_{r,s}|\mu^{r0}|^2|\mu^{s0}|^2\int_0^\infty \frac{k_{r0}k_{s0}}{(k_{r0}^2+u^2)(k_{s0}^2+u^2)}\,\mathrm{d}u. \tag{13.10}$$

With the identity

$$\frac{1}{a+b}=\frac{2}{\pi}\int_0^\infty \frac{ab}{(a^2+u^2)(b^2+u^2)}\,\mathrm{d}u, \quad a,b\geqslant 0, \tag{13.11}$$

the near-zone result can be converted to the well known London interaction energy

$$\Delta E = -\frac{1}{24\pi^2\varepsilon_0^2 R^6}\sum_{r,s}\frac{|\mu^{r0}|^2|\mu^{s0}|^2}{E_{r0}+E_{s0}}. \tag{13.12}$$

An alternative route to dispersion interactions in QED is available in the Heisenberg representation. Our discussion throughout has been in the Schrödinger representation, in which the operators are time-independent, with the time dependence being carried by the state vectors. In the Heisenberg representation time-dependent operators act on time-independent state vectors. In the application to dispersion coupling (Power and Thirunamachandran 1983, Thirunamachandran 1988) Heisenberg operators for the electromagnetic field are calculated in the vicinity of one of the coupled pair of molecules. These operators, evolving in time, act both on the state of the field and on the molecular state. They are applied to the second molecule of the coupled pair, viewed as a test body, and the response of the second molecule leads to the dispersion energy. The results agree with those found in the Schrödinger basis. They apply at all intermolecular separations beyond molecular overlap.

Finally, we discuss another aspect of dispersion interactions. This is that, when acting between chiral molecules, the dispersion force differs according to whether the two molecules have like, or unlike, handedness. This difference is referred to as chiral discrimination (Craig and Mellor 1976, Craig 1978). As noted in section 6, molecular chiral properties depend on both electric and magnetic transition moments, through the optical rotatory tensor with components (for a transition $|t\rangle\leftarrow|0\rangle$) $R_{ij}^{t0}=\mathrm{Im}\,\mu_i^{0t}m_j^{t0}$, where $\mathbf{m}$ is the magnetic moment. In achiral systems no transition can be both electrically and magnetically allowed; hence the optical rotatory tensor is identically zero. Transitions in chiral systems, however, can be simultaneously electric- and magnetic-dipole-allowed, a property that is the origin of chiroptical properties such as circular dichroism, optical rotation and chiral discrimination.

In the discussion so far we have employed the electric dipole approximation. Now we must relax this to take into account magnetic dipole coupling as well. We find that there are additional interaction energies between chiral molecules that depend on the relative handedness of the two molecules. The calculation of discriminatory dispersion energies follows the same lines as those of the Casimir–Polder energy, with the important difference that magnetic terms must be included in H_{int}:

$$H_{\mathrm{int}} = -\varepsilon_0^{-1}\boldsymbol{\mu}(\mathrm{A})\cdot\mathbf{d}(\mathbf{R}_\mathrm{A})-\varepsilon_0^{-1}\boldsymbol{\mu}(\mathrm{B})\cdot\mathbf{d}(\mathbf{R}_\mathrm{B})-\mathbf{m}(\mathrm{A})\cdot\mathbf{b}(\mathbf{R}_\mathrm{A})-\mathbf{m}(\mathrm{B})\cdot\mathbf{b}(\mathbf{R}_\mathrm{B}). \tag{13.13}$$

The time-ordered graphs are also modified by replacing one of the electric dipole interaction vertices at each centre by a magnetic dipole interaction vertex. Details of the calculation may be found elsewhere (Craig 1978, Craig and Thirunamachandran 1984). We present here the results for the two asymptotic limits. In the far zone the discriminatory dispersion energy is

$$\frac{\hbar^3 c}{3\pi^3 \varepsilon_0^2 R^9} \sum_r \frac{R^{r0}}{E_{r0}^2} \sum_s \frac{R^{s0}}{E_{s0}^2}, \tag{13.14}$$

where R^{r0} and R^{s0} are the rotatory strengths (equal to the diagonal sums of R_{ij}^{t0} above) of transitions $|r\rangle \leftarrow |0\rangle$ and $|s\rangle \leftarrow |0\rangle$ in molecules A and B. Since rotatory strength is a pseudoscalar, it is evident that (13.14) changes sign when one molecule of the pair is replaced by its enantiomer.

In the near zone the chiral discriminatory interaction energy (Mavroyannis and Stephen 1962, Craig *et al.* 1971) is

$$\frac{1}{12\pi^2 \varepsilon_0^2 c^2 R^6} \sum_{r,s} \frac{R^{r0} R^{s0}}{E_{r0} + R_{s0}}. \tag{13.15}$$

Again the pseudoscalar nature of the rotatory strength is responsible for the discriminatory property. The form of (13.15) is similar to that of the London expression (13.12) except that the squared moduli of the electric dipole moments are replaced by rotatory strengths. It should be noted that, although the London interaction is always attractive, the discriminatory interaction can be either attractive or repulsive.

14. The two-centre model for circular dichroism

Circular dichroism is a property of chiral molecules. It can be described in terms of the electric and magnetic transition moments for the associated molecular transition (section 6). In an important set of special cases the low-frequency optical properties arise in two (or more) well separated chromophoric centres A and B, held by a rather rigid but spectrally inactive framework. Circular dichroism can then be discussed in terms of the properties of these centres, and of the coupling between them via their individual transitions. There are particular cases of interest where chiral behaviour appears through the coupling of centres that are locally achiral, as for example keto groups in a diketone. The classic illustration is the coupled-oscillator model for optical activity, in which the dissymmetric juxtaposition of two achiral chromophores leads to phenomena associated with chirality of the pair (Kirkwood 1937, Buckingham and Stiles 1974). The overall molecular symmetry must be chiral, with implied constraints on the rigidity of the framework maintaining the relative positions and orientations of A and B.

In another type of two-centre interaction, to be discussed in the next section, coupling is between two *molecules*, one of which is achiral (A) and the other chiral (C). Typically the chiral molecules are the solvent in which A is dissolved. Here the coupling can cause chiral properties to appear in the achiral species, for example circular dichroism at a transition of A. This is *molecule-induced circular dichroism.*

In the two-centre model for circular dichroism the optical response of each centre is effected through its electric transition moment. The spatial displacement of the electric dipoles at the two centres causes a differential response to right- and left-handed light. In the one-centre model, where the molecule is dealt with as one entity, the response involves both electric and magnetic dipole moments of the molecular transition.

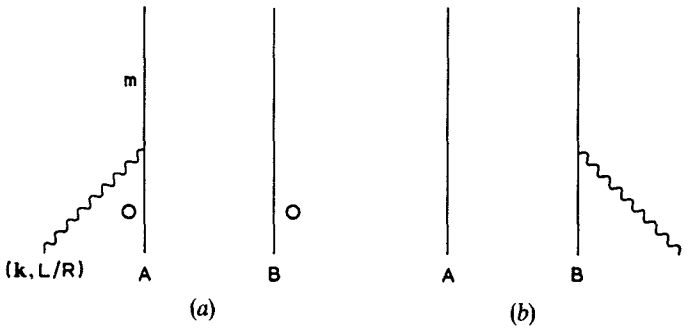

Figure 13. Graphs for two-group circular dichroism with no coupling between the two groups.

The simplest case is the circular dichroism of a pair of identical chromophores A and B. The molecular skeleton simply keeps the relative orientations of the chromophores locked. We may suppose that the transition of interest connects the initial state

$$|\mathrm{i}\rangle = |E_0^{\mathrm{A}}, E_0^{\mathrm{B}}; n(\mathbf{k}, \mathrm{L/R})\rangle, \tag{14.1}$$

with a final state

$$|\mathrm{f}_\pm\rangle = 2^{-1/2}(|E_m^{\mathrm{A}}, E_0^{\mathrm{B}}\rangle \pm |E_0^{\mathrm{A}}, E_m^{\mathrm{B}}\rangle)|(n-1)(\mathbf{k}, \mathrm{L/R})\rangle. \tag{14.2}$$

The states $2^{-1/2}(|E_m^{\mathrm{A}}, E_0^{\mathrm{B}}\rangle \pm |E_0^{\mathrm{A}}, E_m^{\mathrm{B}}\rangle)$ can be split by resonance interaction (section 11), and the spectrum should in general feature a doublet. The leading contribution to the matrix element for the transition $|\mathrm{f}_\pm\rangle \leftarrow |\mathrm{i}\rangle$ is found from the graphs in figure 13. We have

$$M_{\mathrm{fi}}^{(\mathrm{L/R})}(\pm) = 2^{-1/2}[\langle (n-1)(\mathbf{k}, \mathrm{L/R}); E_m^{\mathrm{A}}| -\varepsilon_0^{-1}\boldsymbol{\mu}(\mathrm{A})\cdot\mathbf{d}(\mathbf{R}_{\mathrm{A}})|E_0^{\mathrm{A}}; n(\mathbf{k}, \mathrm{L/R})\rangle$$

$$\pm\langle (n-1)(\mathbf{k}, \mathrm{L/R}); E_m^{\mathrm{B}}| -\varepsilon_0^{-1}\boldsymbol{\mu}(\mathrm{B})\cdot\mathbf{d}(\mathbf{R}_{\mathrm{B}})|E_0^{\mathrm{B}}; n(\mathbf{k}, \mathrm{L/R})\rangle], \tag{14.3}$$

leading to the differential absorption rate

$$\Gamma_\pm^{(\mathrm{L})} - \Gamma_\pm^{(\mathrm{R})} = \frac{\mathscr{I}(\omega)}{4\varepsilon_0\hbar^2}(e_i^{(\mathrm{L})}\bar{e}_j^{(\mathrm{L})} - e_i^{(\mathrm{R})}\bar{e}_j^{(\mathrm{R})})[\mu_i^{m0}(\mathrm{A}) \pm \exp(\mathrm{i}\mathbf{k}\cdot\mathbf{R})\,\mu_i^{m0}(\mathrm{B})]$$

$$\times[\mu_j^{m0}(\mathrm{A}) \pm \exp(-\mathrm{i}\mathbf{k}\cdot\mathbf{R})\,\mu_j^{m0}(\mathrm{B})], \tag{14.4}$$

where $R = |\mathbf{R}_{\mathrm{B}} - \mathbf{R}_{\mathrm{A}}|$. After rotational averaging to take into account tumbling of the pair with respect to the direction of propagation of the incident beam, we obtain

$$\langle\Gamma_\pm^{(\mathrm{L})}\rangle - \langle\Gamma_\pm^{(\mathrm{R})}\rangle = \pm\frac{\mathscr{I}(\omega)}{2\varepsilon_0\hbar^2}\left(\frac{\cos kR}{kR} - \frac{\sin kR}{k^2R^2}\right)[\boldsymbol{\mu}^{m0}(\mathrm{A}) \times \boldsymbol{\mu}^{m0}(\mathrm{B})]\cdot\hat{\mathbf{R}}, \tag{14.5}$$

which gives differential absorption of equal magnitude but opposite sign for each component of the absorption doublet (Craig and Thirunamachandran 1984). The fact that this result arises from interference between matrix elements for absorption at A and at B reflects a chiral response of the pair to variation in the electromagnetic field over the inter-chromophore region. This dichroism must disappear if A and B can rotate freely relative to each other.

While the above result is valid for all distances, the requirement for the two chromophores to be held in a fixed mutual orientation means that R is normally much smaller than optical wavelengths, so that $kR \ll 1$. The result (14.5) then simplifies to

$$\langle \Gamma_{\pm}^{(\mathrm{L})} \rangle - \langle \Gamma_{\pm}^{(\mathrm{R})} \rangle = \mp \frac{\mathscr{I}(\omega)k}{6\varepsilon_0 \hbar^2} [\boldsymbol{\mu}^{m0}(\mathrm{A}) \times \boldsymbol{\mu}^{m0}(\mathrm{B})] \cdot \mathbf{R}, \tag{14.6}$$

showing a linear dependence on R. This result can be also found by treating the coupled A–B pair as a one-centre, inherently dissymmetric system and using the result (6.6) derived previously. With A as the origin, the electric and magnetic dipole moments are

$$\boldsymbol{\mu}(\pm) = 2^{-1/2}[\boldsymbol{\mu}^{m0}(\mathrm{A}) \pm \boldsymbol{\mu}^{m0}(\mathrm{B})], \tag{14.7}$$

$$\mathbf{m}(\pm) = \mp 8^{-1/2} \frac{e}{m} \sum_{\alpha} \mathbf{R} \times \mathbf{p}_{\alpha}^{m0}, \tag{14.8}$$

where the α-sum is over the active electrons of B. With the aid of

$$[\mathbf{q}, H_{\mathrm{B}}] = \frac{\mathrm{i}\hbar}{m} \mathbf{p}, \tag{14.9}$$

$\mathbf{m}(\pm)$ can be written as

$$\mathbf{m}(\pm) = \pm 8^{-1/2} \mathrm{i} \frac{E_{m0}}{\hbar} \mathbf{R} \times \boldsymbol{\mu}^{m0}(\mathrm{B}), \tag{14.10}$$

so that the rotational strength is

$$\begin{aligned} R^{m0}(\pm) &= \mathrm{Im}\, \boldsymbol{\mu}^{0m}(\pm) \cdot \mathbf{m}^{m0}(\pm) \\ &= \mp \tfrac{1}{4} ck [\boldsymbol{\mu}^{m0}(\mathrm{A}) \times \boldsymbol{\mu}^{m0}(\mathrm{B})] \cdot \mathbf{R}. \end{aligned} \tag{14.11}$$

Substitution of (14.11) in (6.6) gives (14.6). Clearly the rotational strength disappears if the two transition moments are parallel or if either is aligned with the **R**-vector. The circular dichroism is almost zero if the two states $|\mathrm{f}_{\pm}\rangle$ are nearly degenerate, since the total differential absorption rate is the sum for the two transitions $|\mathrm{f}_{\pm}\rangle \leftarrow |\mathrm{i}\rangle$. For such cases higher-order contributions containing virtual-photon exchange between the chromophores need to be included, and the calculations are essentially the same as those for non-identical chromophores, which we now consider.

If A and B are different, with different transition frequencies, only one of the diagrams similar to figure 13 can contribute to the transition. Thus there is no

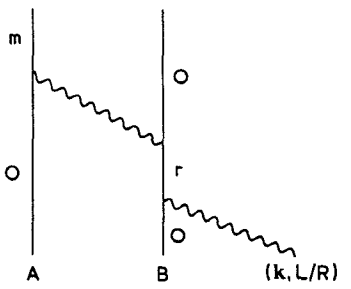

Figure 14. Typical graph for two-group circular dichroism with coupling between the two groups.

interference between first-order amplitudes for absorption at each centre. The interference that leads to circular dichroism now is between first- and third-order contributions to the matrix element.

Let us consider the transition $|m\rangle \leftarrow |0\rangle$ of chromophore A and calculate the circular dichroism arising from the coupling with B. We have for the initial and final states

$$|\mathrm{i}\rangle = |E_0^{\mathrm{A}}, E_0^{\mathrm{B}}; n(\mathbf{k}, \mathrm{L/R})\rangle, \tag{14.12}$$

$$|\mathrm{f}\rangle = |E_m^{\mathrm{A}}, E_0^{\mathrm{B}}; (n-1)(\mathbf{k}, \mathrm{L/R})\rangle. \tag{14.13}$$

The leading contribution to the matrix element, denoted by $M_1^{\mathrm{L/R}}$, comes from the first-order term in (2.14), and is represented by a time-ordered diagram similar to that of figure 13 (*a*). Terms for the third-order perturbation $M_3^{\mathrm{L/R}}$ also contribute, and involve virtual-photon coupling. Six time-ordered diagrams of the type shown in figure 14 contribute. The total matrix element is then a sum

$$M_{\mathrm{fi}}^{\mathrm{L/R}} = M_1^{\mathrm{L/R}} + M_3^{\mathrm{L/R}} + \ldots, \tag{14.14}$$

where

$$M_1^{\mathrm{L/R}} = -\mathrm{i}\left(\frac{n\hbar ck}{2\varepsilon_0 V}\right)^{1/2} \mathbf{e}^{(\mathrm{L/R})}(\mathbf{k}) \cdot \boldsymbol{\mu}^{m0}(\mathrm{A}), \tag{14.15}$$

$$M_3^{\mathrm{L/R}} = \mathrm{i}\left(\frac{n\hbar ck}{2\varepsilon_0 V}\right)^{1/2} e_k^{\mathrm{L/R}}(\mathbf{k}) \mu_i^{m0}(\mathrm{A}) \alpha_{jk}(\mathrm{B}) \times \frac{1}{4\pi\varepsilon_0 R^3} [\beta_{ij}(1 - \mathrm{i}kR) - \alpha_{ij} k^2 R^2] \exp(\mathrm{i}kR). \tag{14.16}$$

In (14.16) α(B) is the dynamic polarizability of B, already defined by (12.4); α_{ij} and β_{ij} are the coupling tensors already defined by (11.5) and (11.6). The absorption rate given by the Fermi rule may be written as

$$\Gamma^{(\mathrm{L/R})} = \frac{2\pi\rho}{\hbar} (|M_1^{\mathrm{L/R}}|^2 + 2\,\mathrm{Re}\, M_1^{\mathrm{L/R}} \bar{M}_3^{\mathrm{L/R}} + \ldots). \tag{14.17}$$

For an achiral A the first-order term in (14.17) does not lead to circular dichroism. The leading contribution to circular dichroism arises from the $M_1 \bar{M}_3$ interference terms, and, after performing a tumbling average for the pair, we obtain

$$\langle \Gamma^{(\mathrm{L})} \rangle - \langle \Gamma^{(\mathrm{R})} \rangle = \frac{\mathscr{I}(\omega)}{8\pi\varepsilon_0^2 \hbar^2 k^2 R^6} \varepsilon_{\nu\pi\tau} \mu_\lambda^{m0}(\mathrm{A}) \mu_\pi^{m0}(\mathrm{A}) \alpha_{\mu\nu}(\mathrm{B}) R_\tau W_{\lambda\mu}(k, \mathbf{R}), \tag{14.18}$$

where

$$W_{\lambda\mu}(k, \mathbf{R}) = \{\beta_{\lambda\mu}[2kR\cos 2kR + (k^2R^2 - 1)\sin 2kR] + \alpha_{\lambda\mu}[k^2R^2 \sin 2kR - k^3R^3(1 + \cos 2kR)]\}. \tag{14.19}$$

In the near-zone ($kR \ll 1$) the first factor of the $\beta_{\lambda\mu}$ term dominates and an overall R^{-5} dependence follows (Craig and Thirunamachandran 1984).

15. Molecule-induced circular dichroism

In section 7 we noted that chirality may be induced in achiral molecules by circularly polarized laser radiation. Chirality can also be induced by a chiral medium so that a transition of an achiral species A shows circular dichroism when A is dissolved in

a chiral solvent C. Here the coupling can result in the induction of chirality in A leading to circular dichroism at a transition frequency of A. For example, n–π* transitions in aromatic ketones dissolved in chiral solvents such as pinene show circular dichroism (Bosnich 1967, Hayward and Totty 1971).

The time-ordered diagrams for this phenomenon are essentially the same as those in figure 14, but with the important difference that the interaction vertices for the chiral centre now include magnetic dipole coupling. This is required because A and C in general have no orientational correlation, and rotational averages have to be performed to take into account not only the tumbling of the pair with respect to the incident beam but also the random relative orientation of the molecules. As a result, any contribution associated with electric dipole-only coupling vanishes, and the induced chirality arises from an inclusion of magnetic dipole terms for the chiral centre. The calculation, though lengthy, is straightforward, and the induced circular dichroism for an arbitrary A–C separation distance R is (Craig *et al.* 1976, Craig and Thirunamachandran 1984)

$$\langle \Gamma_{\mathrm{A}}^{(\mathrm{L})} \rangle - \langle \Gamma_{\mathrm{A}}^{(\mathrm{R})} \rangle = \frac{\mathscr{I} k}{18\pi\hbar\varepsilon_0^2 R^3} |\boldsymbol{\mu}^{m0}(\mathrm{A})|^2 \chi(k, \mathrm{C}) \left[\left(\frac{3}{k^3 R^3} - \frac{4}{kR} \right) \sin 2kR - \frac{6}{k^2 R^2} \cos 2kR \right], \tag{15.1}$$

where

$$\chi(k, \mathrm{C}) = \sum_r \frac{R^{r0}}{E_{r0}^2 - \hbar^2 c^2 k^2}. \tag{15.2}$$

and R^{r0} is the rotational strength given by (6.7). Thus $\chi(k, \mathrm{C})$ represents the complete chiral response of C summed over all its absorption bands, but weighted towards bands of frequencies closest to the absorption frequency $\omega(=ck)$ of A. For $kR \ll 1$ the result (15.1) varies as R^{-1} and thus falls off comparatively slowly with intermolecular distance. The dependence is R^{-1} rather than R^{-3}, the expected dependence of the 'true' static limit, because in this limit there is no coupling between the electric dipole transition moment of A and the magnetic dipole transition moment of C.

It is of interest to note an alternative route to (15.1). Instead of using the coupling of electric and magnetic moments with the displacement vector and the magnetic fields as the primary interaction operators for the chiral centre, it is possible to use an effective interaction operator that is quadratic in the fields. For the calculation of circular dichroism, the effective operator for a freely rotating molecule C is of the form

$$H_{\mathrm{int}}^{\mathrm{eff}} = -\frac{1}{2\varepsilon_0} \sum_{\substack{\mathbf{k}, \mathrm{L/R} \\ \mathbf{p}, \lambda}} G(k, \mathrm{C}) [\mathbf{d}(\mathbf{k}, \mathrm{L/R}) \cdot \mathbf{b}(\mathbf{p}, \lambda) + \mathbf{d}(\mathbf{p}, \lambda) \cdot \mathbf{b}(\mathbf{k}, \mathrm{L/R})], \tag{15.3}$$

where

$$\begin{aligned} G(k) &= \sum_r \left(\frac{\boldsymbol{\mu}^{0r} \cdot \mathbf{m}^{r0}}{E_{r0} - \hbar ck} + \frac{\mathbf{m}^{0r} \cdot \boldsymbol{\mu}^{r0}}{E_{r0} + \hbar ck} \right) \\ &= \mathrm{i}\, 2\hbar ck \chi(k, \mathrm{C}), \end{aligned} \tag{15.4}$$

with χ given by (15.2). The use of effective two-photon operators of the type (15.3) can be understood in terms of canonical transformations (Craig *et al.* 1976). With the aid of the two-photon operator, induced circular dichroism may be visualized as arising from an

interference between the directly absorbed wave at A and the wave scattered by the chiral molecule, the interference depending on the helicity of the incident photons.

Finally, we note that the coupling between the achiral and chiral molecules can lead to changes in the rotatory strengths of the chiral molecule from the free-molecule values. The calculations follow the same lines as above and may be found elsewhere (Craig and Thirunamachandran 1987). Measurements of the changes in the rotatory tensor should provide additional information about the coupling. The most promising is the application to chiral molecules isolated in a rare gas matrix, or embedded in a host crystal of achiral molecules. From studies of such systems it should be possible to learn about the directional properties of active transition moments in the chiral molecule.

16. Synergistic effects in two-photon absorption

The interaction of atoms or molecules irradiated with light of a suitable frequency can result in the simultaneous excitation of two distinct species. Although the first observations of this effect were made in infrared studies in compressed gases, recent studies have mostly focused on interaction-induced *ultraviolet/visible* transitions in gases and crystals. Such pair excitation involves the absorption of a single photon. Laser excitation provides the means for observing nonlinear optical effects in which two or more photons are absorbed by a pair. Such a process was predicted by Rios Leite and De Araujo (1980) in a paper concerned with cooperative absorption by atom pairs in solids. However, the first observation, made shortly afterwards by White (1981), came from laser excitation studies of gaseous mixtures of barium and thallium. Atoms of both species were found to be simultaneously promoted to excited states by a concerted process involving the pairwise absorption of laser photons.

Recently, a new type of synergistic photoabsorption involving *two-frequency* excitation has been the subject of theoretical interest (Andrews and Hopkins 1987, 1988a, b). Here the two chemical centres that undergo concerted excitation may or may not be chemically similar, and can represent either distinct chromophores within a single molecule, loosely bound systems such as van der Waals molecules or solute particles within a coordination shell of solvent molecules, or else completely separate molecules. In the most general case the two centres A and B undergo a concerted excitation through the absorption of two laser photons $\hbar\omega_1$ and $\hbar\omega_2$, and represented by

$$\mathrm{A}+\mathrm{B}+\hbar\omega_1+\hbar\omega_2\rightarrow\mathrm{A}^*+\mathrm{B}^*, \tag{16.1}$$

subject to energy conservation

$$E_{\alpha 0}+E_{\beta 0}=\hbar\omega_1+\hbar\omega_2. \tag{16.2}$$

It is assumed that both molecules A and B are initially in their ground states, and that they are promoted during the absorption process to excited vibronic states denoted by the asterisks in (16.1) and α and β in (16.2).

Synergistic two-photon absorption can in principle take place by one of two mechanisms, where either (i) each laser photon is absorbed by a different centre (the *cooperative* mechanism; Andrews and Harlow (1983)), or (ii) both laser photons are absorbed by a single molecule (the *distributive* mechanism; Andrews and Harlow (1984)). In each case the energy mismatch for the molecular transitions is transferred between the molecules by means of virtual-photon exchange. The result, however, is a significant difference in the selection rules applying to the two types of process.

In the cooperative case the two molecular transitions are separately allowed under standard two-photon selection rules, since each molecule absorbs one laser photon and either emits or absorbs a virtual photon. In a similar manner the distributive case provides for excitation through three- and one-photon allowed transitions, and may thus lead to excitation of states that are formally two-photon forbidden. Since on the whole these processes are of most interest for molecules of high symmetry, it can safely be assumed that in most cases one mechanism alone is involved in the excitation to a particular pair of excited states.

The initial and final states for the process are represented by

$$|\mathrm{i}\rangle = |E_0^{\mathrm{A}}, E_0^{\mathrm{B}}; n_1(\mathbf{k}_1, \lambda_1), n_2(\mathbf{k}_2, \lambda_2)\rangle, \tag{16.3}$$

$$|\mathrm{f}\rangle = |E_\alpha^{\mathrm{A}}, E_\beta^{\mathrm{B}}; (n_1 - 1)(\mathbf{k}_1, \lambda_1), (n_2 - 1)(\mathbf{k}_2, \lambda_2)\rangle, \tag{16.4}$$

where the sequence in the ket denotes: |the state of A, the state of B; the number of photons in beam 1, the number of photons in beam 2⟩. The complete set of interaction sequences incorporated in the fourth-order term for M_{fi} is accounted for by 96 time-ordered diagrams, 48 of which are associated with the cooperative mechanism and 48 with the distributive mechanism; examples of each type are shown in figure 15. Of the distributive type, 24 diagrams correspond to the case where both real photons are absorbed at centre A, with a virtual photon conveying the energy mismatch to B; the other 24 correspond to the case where both real photons are absorbed at B, together with virtual photon exchange between A and B. The addition of all 96 matrix element contributions gives the complete fourth-order result for M_{fi}.

The matrix element for the absorption may be expressed in terms of the molecular tensors S_{ij} and χ_{ijk}:

$$\begin{aligned} M_{\mathrm{fi}} = -\frac{\hbar c}{2\varepsilon_0 V}(n_1 n_2 k_1 k_2)^{1/2} e_{1i} e_{2j} \\ \times \{ & S_{ik}^{\alpha 0}(\omega_1) S_{jl}^{\beta 0}(\omega_2) V_{kl}[(\omega_{\beta 0} - \omega_2), \mathbf{R}] \exp[\mathrm{i}(\mathbf{k}_1 \cdot \mathbf{R}_{\mathrm{A}} + \mathbf{k}_2 \cdot \mathbf{R}_{\mathrm{B}})] \\ & + S_{ik}^{\beta 0}(\omega_1) S_{jl}^{\alpha 0}(\omega_2) V_{kl}[(\omega_{\beta 0} - \omega_1), \mathbf{R}] \exp[\mathrm{i}(\mathbf{k}_2 \cdot \mathbf{R}_{\mathrm{A}} + \mathbf{k}_1 \cdot \mathbf{R}_{\mathrm{B}})] \\ & + \chi_{ijk}^{\alpha 0}(\omega_1, \omega_2) \mu_l^{\beta 0} V_{kl}(\omega_{\beta 0}, \mathbf{R}) \exp[\mathrm{i}(\mathbf{k}_1 + \mathbf{k}_2) \cdot \mathbf{R}_{\mathrm{A}}] \\ & + \chi_{ijk}^{\beta 0}(\omega_1, \omega_2) \mu_l^{\alpha 0} V_{kl}(\omega_{\alpha 0}, \mathbf{R}) \exp[\mathrm{i}(\mathbf{k}_1 + \mathbf{k}_2) \cdot \mathbf{R}_{\mathrm{B}}] \}, \end{aligned} \tag{16.5}$$

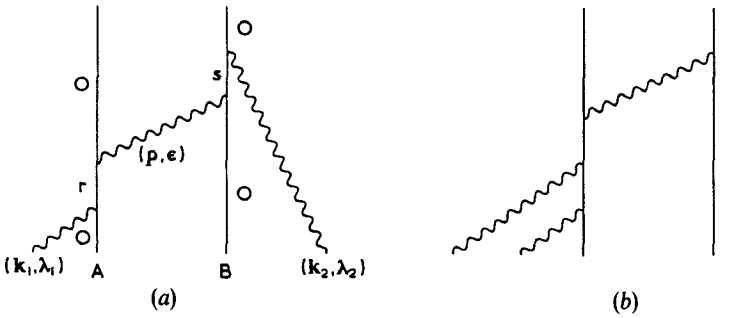

Figure 15. Typical graphs for two-photon absorption by two interacting centres: (*a*) represents cooperative absorption, (*b*) distributive absorption.

where the first two terms arise from the cooperative mechanism and the last two from the distributive mechanism. In (16.5) $\mathbf{R}_A$ and $\mathbf{R}_B$ are the position vectors of A and B, and $\mathbf{R}=\mathbf{R}_B-\mathbf{R}_A$; the tensor V_{kl} is the retarded resonance dipole–dipole coupling:

$$V_{kl}(\omega,\mathbf{R})=\frac{1}{4\pi\varepsilon_0 R^3}[\beta_{kl}(1+ikR)-\alpha_{kl}k^2R^2]. \tag{16.6}$$

The explicit form of the second-rank molecular response tensor is

$$S_{ij}^{f0}(\omega)=\sum_r\left(\frac{\mu_i^{fr}\mu_j^{r0}}{E_{rf}+\hbar\omega}+\frac{\mu_j^{fr}\mu_i^{r0}}{E_{r0}-\hbar\omega}\right). \tag{16.7}$$

This tensor is the same as the electronic Raman scattering tensor for the Raman transition $|f\rangle\leftarrow|0\rangle$. The third-rank molecular tensor χ_{ijk}^{f0} is defined by

$$\begin{aligned}\chi_{ijk}^{f0}=\sum_{r,s}\Bigg[&\frac{\mu_i^{fs}\mu_j^{sr}\mu_k^{r0}}{(E_{rf}+\hbar\omega_1+\hbar\omega_2)(E_{sf}+\hbar\omega_1)}+\frac{\mu_i^{fs}\mu_k^{sr}\mu_j^{r0}}{(E_{r0}-\hbar\omega_2)(E_{sf}+\hbar\omega_1)}\\&+\frac{\mu_k^{fs}\mu_i^{sr}\mu_j^{r0}}{(E_{s0}-\hbar\omega_1-\hbar\omega_2)(E_{r0}-\hbar\omega_2)}+\frac{\mu_j^{fs}\mu_i^{sr}\mu_k^{r0}}{(E_{rf}+\hbar\omega_1+\hbar\omega_2)(E_{sf}+\hbar\omega_2)}\\&+\frac{\mu_j^{fs}\mu_k^{sr}\mu_i^{r0}}{(E_{sf}+\hbar\omega_2)(E_{r0}-\hbar\omega_1)}+\frac{\mu_k^{fs}\mu_j^{sr}\mu_i^{r0}}{(E_{s0}-\hbar\omega_1-\hbar\omega_2)(E_{r0}-\hbar\omega_1)}\Bigg].\end{aligned} \tag{16.8}$$

There are four specific cases of bimolecular mean-frequency absorption that are of special interest. These are distinguished by the type of mechanism (cooperative or distributive) involved, and whether the photons absorbed have the same or different frequencies. The latter condition is in most cases determined by whether a single laser beam or two laser beams are employed for the excitation.

We first consider the single-beam cases. Here the two absorbed photons have the same frequency, and it is the synergistic interaction between two *non-identical* centres that is of interest. This interaction provides the mechanism for energy exchange such that an overall process

$$A+B+2\hbar\omega\rightarrow A^*+B^*. \tag{16.9}$$

can take place even when the individual transitions $A^*\leftarrow A$ and $B^*\leftarrow B$ are forbidden on energy grounds. From a phenomenological viewpoint, the process evidently has the characteristics of *mean-frequency* absorption. For this effect to be experimentally observable, ω must be chosen to lie in a region where neither A nor B displays absorption, and we thus have

$$\hbar\omega=\tfrac{1}{2}(E_{\alpha 0}+E_{\beta 0}), \tag{16.10}$$

$$\hbar\omega\neq E_{\alpha 0}, E_{\beta 0}. \tag{16.11}$$

So, for two chemically distinct molecules or chromophores A and B, with well characterized vibronic excited states α and β, a proximity-induced two-photon absorption process can be effected by tuning the exciting laser to a frequency equivalent to a *mean* of the frequencies for the two transitions.

In fluid phases it is necessary to take account of molecular tumbling on the absorption rate. Two distinct cases arise. In the first the relative orientation of the two centres A and B is fixed, but the A–B pair is free to tumble with respect to the laser beam. The result thereby obtained is applicable to van der Waals molecules and to

polyatomic molecules in which A and B are independent chromophores. For single-beam cooperative two-photon absorption by a rotating pair the rate expression is

$$\begin{aligned}\langle \Gamma_{1c} \rangle = &\frac{\pi\hbar c^2 \rho_f}{60\varepsilon_0^2 V^2} n_1 n_2 k_1 k_2 V_{kl}(\omega_{\beta 0} - \omega, \mathbf{R}) \bar{V}_{op}(\omega_{\beta 0} - \omega, \mathbf{R}) \\ &\times [(4|\mathbf{e}\cdot\mathbf{e}|^2 - 2) S_{ik}^{\alpha 0}(\omega) S_{jl}^{\beta 0}(\omega) \bar{S}_{jo}^{\alpha 0}(\omega) \bar{S}_{ip}^{\beta 0}(\omega) \\ &\quad - (|\mathbf{e}\cdot\mathbf{e}|^2 - 3) S_{ik}^{\alpha 0}(\omega) S_{jl}^{\beta 0}(\omega) \bar{S}_{io}^{\alpha 0}(\omega) \bar{S}_{jp}^{\beta 0}(\omega) \\ &\quad - (|\mathbf{e}\cdot\mathbf{e}|^2 - 3) S_{ik}^{\alpha 0}(\omega) S_{jl}^{\beta 0}(\omega) \bar{S}_{jo}^{\alpha 0}(\omega) \bar{S}_{ip}^{\beta 0}(\omega)], \end{aligned} \tag{16.12}$$

where the angular brackets around Γ_{1c} signify the averaged result. The polarization product $\mathbf{e}\cdot\mathbf{e}$ takes the limiting values of zero for circularly polarized light and unity for plane-polarized light. Where the two molecules involved in the interaction are free to take up any mutual orientation, a further average is required to take account of the random relative orientation of the two molecules. The final result displays precisely the same change from near-zone R^{-6} to far-zone R^{-2} behaviour mentioned earlier in connection with resonance energy transfer (cf. (11.9)). The results for single-beam distributive absorption are much more complicated because of the interference of radiation phase factors.

In the other cases of interest the two centres have identical chemical composition and are excited by the absorption of two different photons, as for example from two different laser beams with frequencies ω_1 and ω_2. This process can be represented by

$$\mathrm{A} + \mathrm{A} + \hbar\omega_1 + \hbar\omega_2 \rightarrow \mathrm{A}^* + \mathrm{A}^*. \tag{16.13}$$

Again, for the synergistic process to be observable, the frequencies ω_1 and ω_2 must be in a region where single-photon absorption cannot lead to the excitation of either centre. Thus we have

$$\tfrac{1}{2}(\hbar\omega_1 + \hbar\omega_2) = E_{\alpha 0}, \tag{16.14}$$

$$\hbar\omega_1, \hbar\omega_2 \neq E_{\alpha 0}. \tag{16.15}$$

The relation (16.14) indicates that this cooperative process again has the characteristics of mean-frequency absorption: here, however, it is the molecular excitation frequency that is equal to the mean of the two photon frequencies. Detailed results for these other cases are appreciably more complicated, owing once again to interference between matrix element terms having different radiation phase factors. As in the single-beam case, the same forms of limiting near-zone and far-zone behaviour ensue.

Interesting differences between the cooperative and distributive mechanisms arise in connection with the extent of the near zone, however, especially when the excited-state energies are large but similar. Figure 16 illustrates this point with a log–log plot of the general function $V_{ij}(ck, \mathbf{R})\bar{V}_{ij}(ck, \mathbf{R})$ that occurs in the fully averaged rate expressions. The upper curve is plotted for a value of $k = 1{\cdot}6 \times 10^7\ \mathrm{m}^{-1}$, corresponding to distributive conveyance of an electronic energy $E_{\beta 0}$ with a wavelength of about 400 nm. The lower curve with $k = 8 \times 10^5\ \mathrm{m}^{-1}$ corresponds to the cooperative mechanism where only an electronic energy difference (nominally $\frac{1}{20}E_{\beta 0}$) is conveyed; here the difference equates to a vibrational energy with a wavenumber of around $1250\ \mathrm{cm}^{-1}$. At short distances the two graphs are indistinguishable and display the near-zone R^{-6} dependence. However, the extent of the near zone for the former case is much shorter, with the limiting far-zone R^{-2} behaviour already established at $R = 1\ \mu\mathrm{m}$; for the latter case far-zone behaviour obtains at $R = 10\ \mu\mathrm{m}$. The result of

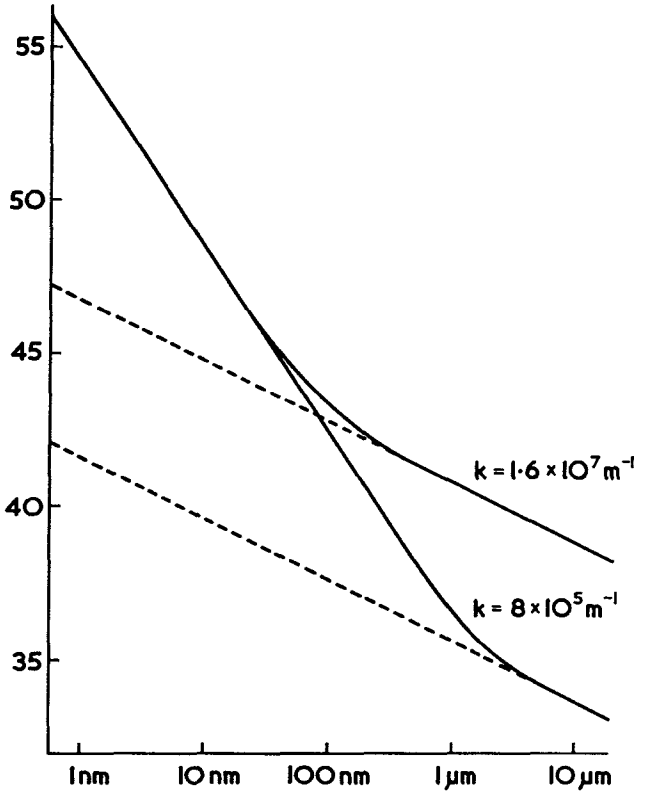

Figure 16. Typical log–log plot of excitation transfer against intermolecular separation.

this difference is that the long-range rates (which vary with k^4) differ by a factor of $20^4 = 160\,000$ in favour of the distributive mechanism, where selection rules permit (Andrews 1989b).

The explicit characterization of synergistic single-beam two-photon absorption has recently been described by Fajardo *et al.* (1988) in connection with a study of laser-induced charge-transfer reactions in solution. Here a clear distinction from the effects of any *sequential* absorption has been made on the basis of kinetic considerations, and it has been shown that the synergistic two-photon absorption mechanism satisfactorily accounts for all the experimental observations.

While the effects of interest are readily studied by specifically designed two-beam laser experiments, the mechanism involved may play a significant role in other photoabsorption processes where optical nonlinearity is not immediately apparent. This is particularly the case in connection with studies based on white or broadband light, and the effects may be manifest in the appearance of anomalous features in the corresponding absorption spectra, especially those obtained using ultrashort laser pulses (Andrews 1988).

Consider a single-photon optical transition $|f\rangle \leftarrow |i\rangle$. When observed with broadband radiation, it is possible to induce this transition in *two* molecules by synergistic absorption. For *cooperative* absorption two photons with frequencies

$\omega = \omega_0 + \Omega$ and $\omega' = \omega_0 - \Omega$, the sum of whose energies is equal to the sum of the $|f\rangle \leftarrow |i\rangle$ transition energies for two different molecules, are absorbed in the concerted process. The rate of cooperative absorption by the pair is

$$\Gamma_{2c} = \frac{\pi}{2\hbar^2 c^2 \varepsilon_0^2} \int_0^\infty K_{2c}(\omega_0, \Omega) \mathcal{I}(\omega_0 + \Omega) \mathcal{I}(\omega_0 - \Omega) \, d\Omega, \tag{16.16}$$

where

$$K_{2c}(\omega_0, \Omega) = |e_i e_j S^{fi}_{ik}(\omega_0 + \Omega) S^{fi}_{jl}(\omega_0 - \Omega)[V_{kl}(\Omega, \mathbf{R}) + \bar{V}_{kl}(\Omega, \mathbf{R}) \exp(i \Delta\mathbf{k} \cdot \mathbf{R})]|^2. \tag{16.17}$$

and $\Delta\mathbf{k} = \mathbf{k}_1 - \mathbf{k}_2$. In the *distributive* mechanism two photons with frequencies $\omega_0 + \Omega$ and $\omega_0 - \Omega$ undergo concerted absorption at the same centre, and the energy mismatch E_{fi} is conveyed to another molecule by virtual photon coupling. For this case the following rate expression is obtained:

$$\Gamma_{2d} = \frac{\pi}{2\hbar^2 c^2 \varepsilon_0^2} \int_0^\infty K_{2d}(\omega_0, \Omega) \mathcal{I}(\omega_0 + \Omega) \mathcal{I}(\omega_0 - \Omega) \, d\Omega, \tag{16.18}$$

where

$$K_{2d}(\omega_0, \Omega) = |e_i e_j \chi^{fi}_{(ij)k}(\omega_0 + \Omega, \omega_0 - \Omega) \mu^{fi}_i V_{kl}(\omega_0, \mathbf{R})[1 + \exp(i\mathbf{u} \cdot \mathbf{R})]|^2, \tag{16.19}$$

with $\mathbf{u} = \mathbf{k}_1 + \mathbf{k}_2$. The Beer–Lambert exponential decay law for conventional single-photon absorption results from the elementary relation

$$-\frac{d\mathcal{I}(\omega, z)}{dz} \propto \mathcal{I}(\omega, z), \tag{16.20}$$

where z is the distance the light has travelled through the sample, which is directly proportional to the transit time within the sample. When intense continuum light is absorbed, however, cooperative and distributive processes produce a correction term, which necessitates the replacement of (16.20) by a result of the form

$$-\frac{d\mathcal{I}(\omega, z)}{dz} \propto \mathcal{I}(\omega, z) + \frac{\chi}{c^2 \varepsilon_0^2 a_0^2 \hbar} \int K(\omega, \Omega) \mathcal{I}(\omega + \Omega, z) \mathcal{I}(\omega - \Omega, z) \, d\Omega, \tag{16.21}$$

where $K = K_{2c} + K_{2d}$. The dimensionless parameter χ is defined by

$$\chi = \frac{c\varepsilon_0 \hbar a_0^2}{2|\boldsymbol{\mu}^{fi} \cdot \mathbf{e}|^2}, \tag{16.22}$$

whose typical value is not far away from unity. Clearly in this case exponential decay is no longer to be expected. Although other sources of optical non-linearity can contribute further correction terms to (16.21), these are all associated with higher powers of the beam intensity.

A significant implication of this result is that an absorption spectrum measured with intense white light may be significantly different from the spectrum that would be observed using tunable monochromatic radiation. In particular, there should be a decrease in the apparent width of many lines in any absorption spectrum measured with broadband radiation. This is because for a transition of frequency ω_0 photons of appreciably off-resonant frequency $\omega_0 \pm \Omega$ can be cooperatively absorbed and result in the excitation of two separate molecules, provided that selection rules permit. In

conclusion, not only intensity-dependent lineshapes or extinction coefficients but also the appearance of ostensibly extraneous spectral lines may all be attributable to the effects of synergistic two-photon absorption.

17. Conclusion

The growing importance of molecular QED in chemical physics rests as much on the physical insight that it provides into processes and mechanisms as on the convenient and straightforward calculations of matrix elements, energy shifts in stationary states, and rates of time-dependent phenomena. Interactions between molecules and radiation, and between molecules and other molecules, are transparently interpreted as combinations of the primitive events of absorption and emission of real and virtual photons in single steps. In radiation–molecule interactions photons are exchanged between the field and the molecule, the dynamics of both being taken into account. In molecule–molecule interactions the coupling is entirely conveyed by transverse photons, with no direct (electrostatic) term. The combination of good insight and convenient calculation owes much to the use of time-ordered diagrams, which are a powerful aid to grasping the underlying physics, with particular advantage in higher-order perturbations.

Quantization of the radiation field, with the associated zero-point (vacuum) energy, explains phenomena beyond the reach of the semi-classical method. As new discoveries are made, especially in the regime of non-linear molecular response to intense laser radiation, the attraction of these methods becomes more evident; the trend towards their increasing use seems certain to continue.

References

ANDREWS, D. L., 1988, *Phys. Rev.* A, **38**, 5129; 1989a, *Chem. Phys.*, **135**, 195; 1989b, *Phys. Rev.* A, **40**, 3431.

ANDREWS, D. L., and BLAKE, N. P., 1988, *Phys. Rev.* A, **38**, 3113.

ANDREWS, D. L., BLAKE, N. P., and HOPKINS, K. P., 1988, *J. chem. Phys.*, **88**, 6022.

ANDREWS, D. L., and HARLOW, M. J., 1983, *J. chem. Phys.*, **78**, 1088; 1984, *Ibid.*, **80**, 4753.

ANDREWS, D. L., and HOPKINS, K. P., 1987, *J. chem. Phys.*, **86**, 2453; 1988a, *J. molec. Struct.*, **175**, 141; 1988b, *J. chem. Phys.*, **88**, 6030.

ANDREWS, D. L., and SHERBORNE, B. S., 1984, *Chem. Phys.*, **88**, 1; 1986, *Ibid.*, **108**, 357; 1987, *J. chem. Phys.*, **86**, 4011.

ANDREWS, D. L., and THIRUNAMACHANDRAN, T., 1977, *J. chem. Phys.*, **67**, 5026.

BOSNICH, B., 1967, *J. Am. chem. Soc.*, **89**, 6143.

BUCKINGHAM, A. D., and STILES, P. J., 1974, *Accts chem. Res.*, **7**, 258.

CARRUTHERS, P., and NIETO, M. M., 1968, *Rev. mod Phys.*, **40**, 411.

CASIMIR, H. B. G., and POLDER, D., *Phys. Rev.*, **73**, 360.

CHEMLA, D. S., and ZYSS, J., 1987, *Optical Properties of Organic Molecules and Crystals*, Vol. 1 and 2 (New York: Academic).

CONDON, E. U., 1932, *Phys. Rev.*, **41**, 759.

CRAIG, D. P., 1978, *Optical Activity and Chiral Discrimination* edited by S. F. Mason (Dordrecht: Reidel), p. 293; 1989, *Perspectives in Quantum Chemistry*, edited by B. Pullman and J. Jortner (Dordrecht: Reidel), p. 19.

CRAIG, D. P., and MELLOR, D. P., 1976, *Topics curr. Chem.*, **63**, 1.

CRAIG, D. P., and POWER, E. A., 1969, *Int. J. quant. Chem.*, **3**, 903.

CRAIG, D. P., POWER, E. A., and THIRUNAMACHANDRAN, T., 1971, *Proc. R. Soc. Lond.* A, **322**, 165.

CRAIG, D. P., and THIRUNAMACHANDRAN, T., 1982, *Adv. quant. Chem.*, **16**, 97; 1984, *Molecular Quantum Electrodynamics* (London: Academic); 1986, *Accts chem. Res.*, **19**, 10; 1987, *Proc. R. Soc. Lond.* A, **410**, 337; 1989, *Chem. Phys.*, **135**, 37.

CRAIG, D. P., and WALMSLEY, S. H., 1967, *Excitons in Molecular Crystals* (New York: Benjamin).

DELSART, C., and KELLER, J.-C., 1978, *J. appl. Phys.*, **49**, 3662.

DIRAC, P. A. M., 1927, *Proc. R. Soc. Lond.* A, **114,** 243.
FAJARDO, M. E., WITHNALL, R., FELD, J., OKADA, F., LAWRENCE, W., WIEDEMAN, L., and APKARIAN, V. A., 1988, *Laser Chem.*, **9,** 1.
FEYNMAN, R. P., 1985, *QED. The Strange Theory of Light and Matter* (Princeton University Press).
GLAUBER, R. J., 1963, *Phys. Rev.*, **131,** 2766.
HAYWARD, L. D., and TOTTY, R. N., 1971, *Can. J. Chem.*, **49,** 624.
HEALY, W. P., 1982, *Non-Relativistic Quantum Electrodynamics* (New York: Academic).
HEITLER, W., 1954, *Quantum Theory of Radiation* (Oxford University Press), p. 41.
HIRSCHFELDER, J. O., 1966, *J. chem. Ed.*, **43,** 451.
HULET, G., HILFER, E. S., and KLEPPNER, D., 1985, *Phys. Rev. Lett.*, **55,** 2137.
KIRKWOOD, J. G., 1937, *J. chem. Phys.*, **5,** 479.
LAM, Y. T., and THIRUNAMACHANDRAN, T., 1982, *J. chem. Phys.*, **77,** 3810.
LORRAIN, P., and CORSON, D. R., 1970, *Electromagnetic Fields and Waves* (San Francisco: Freeman).
MCCLAIN, W. M., 1974, *Accts chem. Res.*, **7,** 129.
MAVROYANNIS, C., and STEPHEN, M. J., 1962, *Molec. Phys.*, **5,** 629.
POWER, E. A., 1964, *Introductory Quantum Electrodynamics* (London: Academic).
POWER, E. A., and THIRUNAMACHANDRAN, T., 1974, *J. chem. Phys.*, **60,** 3695; 1983, *Phys. Rev.* A, **28,** 2671; 1986, *Int. Rev. phys. Chem.*, **5,** 273.
POWER, E. A., and ZIENAU, S., 1957, *Nuovo Cim.*, **6,** 7.
RIOS LEITE, J. R., and DE ARAUJO, C. B., 1980, *Chem. Phys. Lett.*, **73,** 71.
SCHWINGER, J. (editor), 1958, *Quantum Electrodynamics* (New York: Dover).
SHELTON, D. P., and BUCKINGHAM, A. D., 1982, *Phys. Rev.* A, **26,** 2787.
SHEN, Y. R., 1984, *The Principles of Nonlinear Optics* (New York: Wiley).
TABOR, D., and WINTERTON, R. H. S., 1969, *Proc. R. Soc. Lond.* A, **312,** 435.
THIRUNAMACHANDRAN, T., 1979, *Proc. R. Soc. Lond.* A, **365,** 327; 1988, *Physica scripta* T, **21,** 123.
WHITE, J. C., 1981, *Optics Lett.*, **6,** 242.